Since January 2020 Elsevier has created a COVID-19 resource centre with free information in English and Mandarin on the novel coronavirus COVID-19. The COVID-19 resource centre is hosted on Elsevier Connect, the company's public news and information website.

Virus Research 206 (2015) 120–133

Contents lists available at ScienceDirect

Virus Research

journal homepage: www.elsevier.com/locate/virusres

Review

The structure and functions of coronavirus genomic 3′ and 5′ ends

Dong Yang[a], Julian L. Leibowitz[b,*]

[a] Department of Microbiology, Immunology & Biochemistry, The University of Tennessee Health Science Center College of Medicine, Memphis, TN 38163, USA
[b] Department of Microbial Pathogenesis and Immunology, Texas A&M University, College of Medicine, College Station, TX 77843-1114, USA

ARTICLE INFO

Article history:
Available online 28 February 2015

Keywords:
Coronaviruses
RNA secondary structure
cis-Acting sequences
Virus replication
RNA binding proteins

ABSTRACT

Coronaviruses (CoVs) are an important cause of illness in humans and animals. Most human coronaviruses commonly cause relatively mild respiratory illnesses; however two zoonotic coronaviruses, SARS-CoV and MERS-CoV, can cause severe illness and death. Investigations over the past 35 years have illuminated many aspects of coronavirus replication. The focus of this review is the functional analysis of conserved RNA secondary structures in the 5′ and 3′ of the betacoronavirus genomes. The 5′ 350 nucleotides folds into a set of RNA secondary structures which are well conserved, and reverse genetic studies indicate that these structures play an important role in the discontinuous synthesis of subgenomic RNAs in the betacoronaviruses. These *cis*-acting elements extend 3′ of the 5′UTR into ORF1a. The 3′UTR is similarly conserved and contains all of the *cis*-acting sequences necessary for viral replication. Two competing conformations near the 5′ end of the 3′UTR have been shown to make up a potential molecular switch. There is some evidence that an association between the 3′ and 5′UTRs is necessary for subgenomic RNA synthesis, but the basis for this association is not yet clear. A number of host RNA proteins have been shown to bind to the 5′ and 3′ *cis*-acting regions, but the significance of these in viral replication is not clear. Two viral proteins have been identified as binding to the 5′ *cis*-acting region, nsp1 and N protein. A genetic interaction between nsp8 and nsp9 and the region of the 3′UTR that contains the putative molecular switch suggests that these two proteins bind to this region.

Contents

* Corresponding author at: Department of Microbial Pathogenesis and Immunology, Texas A&M University, College of Medicine, 407 Reynolds Medical Building, 1114 TAMU, College Station, TX 77843-1114, USA. Tel.: +1 979 436 0313; fax: +1 979 845 3479.
E-mail address: jleibowitz@tamu.edu (J.L. Leibowitz).

http://dx.doi.org/10.1016/j.virusres.2015.02.025
0168-1702/

1. Introduction

Coronaviruses (CoVs) are an important cause of illness in humans and animals. Most human coronaviruses commonly cause relatively mild respiratory illnesses; however two zoonotic coronaviruses, SARS-CoV and MERS-CoV, can cause severe illness and death. Investigations over the past 35 years have illuminated many aspects of coronavirus replication. The focus of this review is the structural and functional analyses of conserved RNA secondary structures in the 5′ and 3′ of the betacoronavirus genomes.

1.1. Classification and pathogenicity of coronaviruses

Coronaviruses belong to the subfamily Coronavirinae (http://ictvonline.org/virusTaxonomy.asp?version=2012), which together with Torovirinae make up the Coronaviridae family in the order Nidovirales. The Coronavirinae are classified into four genera Alphacoronavirus, Betacoronavirus, Deltacoronavirus and Gammacoronavirus. Torovirinae includes two genera, Torovirus and Bafinivirus. The Coronaviridae comprises a group of evolutionary related single-stranded, positive-sense, non-segmented, enveloped RNA viruses of vertebrates. The RNA genomes are 25–31 kb, the largest genomes of all known RNA viruses, and are infectious when introduced into permissive cells. However, unlike those of almost all other positive-strand RNA viruses, the RNA infectivity of transfected coronavirus genomes is greatly increased in the presence of a source of N protein (Casais et al., 2001; Grossoehme et al., 2009; Yount et al., 2000). Alphacoronaviruses include alphacoronavirus 1 (transmissible gastroenteritis virus, TGEV), porcine epidemic diarrhea virus (PEDV), bat coronavirus 1, BtCoV 512, BtCoV-HKU8, BtCoV-HKU2, human coronavirus HCoV-NL63 and HCoV-229E. Gammacoronaviruses include avian coronavirus and whale coronavirus SW1. Deltacoronaviruses include coronavirus HKU11, HKU12, and HKU13. The major emphasis of this review is on the betacoronaviruses, which has been the most studied genus. Within the genus Betacoronavirus, four lineages (A, B, C, and D) each with a unique set of accessory genes are commonly recognized. Lineage A includes HCoV-OC43 and HCoV-HKU1, betacoronavirus 1 (more commonly known as bovine coronavirus, BCoV), murine coronavirus (MHV); Lineage B includes severe acute respiratory syndrome-related SARS-CoV and various species recovered from bats; Lineage C includes Tylonycteris bat coronavirus HKU4 (BtCoV-HKU4), Pipistrellus bat coronavirus HKU5 (BtCoV-HKU5). Since April 2012, the Middle East Respiratory Syndrome MERS-CoV has emerged as a new member in lineage C of the betacoronaviruses, closely related to bat coronaviruses HKU4 and HKU5 (de Groot et al., 2013; Drexler et al., 2014; Zaki et al., 2012). MERS-CoV is the first Betacoronavirus lineage C member isolated from humans. Lineage D includes Rousettus bat coronavirus HKU9 (BtCoV-HKU9), which has only been detected in bats (http://www.ecdc.europa.eu/en/publications/Publications/novel-coronavirus-rapid-risk-assessment-update.pdf).

Coronaviruses (CoVs) cause respiratory, enteric, hepatic and neurological diseases in a broad range of vertebrate species (Stadler et al., 2003; Weiss and Leibowitz, 2007). Most human coronaviruses commonly cause relatively mild respiratory disease, however two coronaviruses, SARS-CoV (Rota et al., 2003) and MERS-CoV (Zaki et al., 2012) can cause severe illness and death. SARS-CoV was first recognized in China in November 2002 causing a worldwide outbreak including 774 deaths from 2002 to 2003. MERS-CoV is a novel coronavirus first reported in Saudi Arabia in 2012 and has caused illness in hundreds of people from several countries (http://www.cdc.gov/coronavirus/about/index.html). As of July 23, 2014, 837 laboratory-confirmed cases of MERS-CoV infection have been reported by WHO, including 291 deaths. Both SARS-CoV and MERS-CoV are thought to have originated in bats and spread to humans through intermediate hosts (Coleman and Frieman, 2014). Human coronaviruses also have been detected in human CNS and are able to replicate in CNS derived cells (Arbour et al., 1999; Murray et al., 1992) as well as having been isolated from patients with gastroenteritis and diarrhea (Gerna et al., 1985; Resta et al., 1985), and more seriously, causing neonatal necrotizing enterocolitis (Rousset et al., 1984).

2. Genome organization and replication

2.1. Genome organization

Coronaviruses are roughly spherical with a fringe of large, bulbous surface projections. Coronaviruses infect cells primarily by binding of the spike protein to its host specific cell receptors (Delmas et al., 1992; Hofmann et al., 2005; Li et al., 2003; Raj et al., 2013; Williams et al., 1991; Yeager et al., 1992). Virus enters cells by fusion at the cell surface or by an endocytotic pathway depending upon the strain of virus and the target cell (Nash and Buchmeier, 1997; Wang et al., 2008). After entering the cytoplasm and uncoating, the virus particle releases the RNA genome. For all coronaviruses the genomes are organized into 5′ non-structural protein coding regions comprising the replicase genes, which are two-thirds of the genome, and 3′ structural and nonessential accessory protein coding regions (Masters, 2006). Infected cells contain seven to nine virus specific mRNAs with coterminal 3′ ends, the largest of which is the genomic RNA (Masters, 2006). All of the mRNAs carry identical 70–90 nts leader sequences at their 5′ ends (Lai et al., 1983, 1984; Leibowitz et al., 1981; Spaan et al., 1982). The 3′ end of the leader sequence contains the transcriptional regulatory sequence (TRS-L), which is also present in the genome just upstream of the coding sequence for each transcription unit [TRS-B (body)], where it acts as a *cis*-regulator of transcription (Budzilowicz et al., 1985). All coronavirus TRSs include conserved 6–8 nucleotides core sequence (CS) plus variable 5′ and 3′ flanking sequences (Sola et al., 2005). Betacoronaviruses contain a consensus heptameric sequence, 5′-UCUAAAC-3′, with the SARS-CoV TRS having 5′-ACGAAC-3′ as the core sequence (Marra et al., 2003; Rota et al., 2003). Replication occurs shortly after entry and uncoating of the virion through production of full-length genomic and subgenomic negative strand intermediates (Baric and Yount, 2000; Sawicki and Sawicki, 1990; Sethna et al., 1989). Translation of subgenomic mRNAs gives rise to structural and nonstructural viral proteins. The replicated RNA genome is then encapsidated and packaged into virions. A minimal 69-nts packaging signal has been characterized in MHV that maps within ORF1b approximately 20 kb from the 5′ end of the genome, which is sufficient for RNA to be incorporated into virions (Fosmire et al., 1992; Kuo and Masters,

2013; Makino et al., 1990; Narayanan et al., 2003; van der Most et al., 1991). The BCoV packaging signal Exhibits 74% sequence identity to the MHV packaging signal and is located in a similar position (Cologna and Hogue, 2000). The TGEV packaging signal was originally mapped to the first 649 nts at the 5′ end of the genome; subsequently this position was further delimited to the first 598 nts (Escors et al., 2003; Morales et al., 2013). Viruses bud into smooth walled vesicles in the endoplasmic reticulum–Golgi intermediate compartment (*ERGIC*). After budding, virus particles mature in the Golgi, with a compact, electron-dense internal core. Viruses traverse the Golgi and are transported in exocytic vesicles which eventually fuse with the plasma membrane to release virus into the extracellular space (Holmes and Lai, 1996).

2.2. Genomic and subgenomic mRNAs and their encoded proteins

Coronavirus messenger RNA 1, which is genome length, containing two overlapping reading frames ORF 1a and 1b, directs the synthesis of two precursor polyproteins pp1a and pp1ab, *via* a −1 frameshifting mechanism involving a pseudoknot structure (Bredenbeek et al., 1990). The polyproteins are then processed by two or three virus-encoded (in ORF1a) proteinase domains to produce a membrane-bound replicase-transcriptase complex (Brockway et al., 2003). Upon proteolytic processing, the frameshifted ORF 1ab polypeptide generates 15–16 nonstructural proteins, many of which are involved in either RNA synthesis or proteolytic processing required for viral replication: nsp1–nsp11 encoded in ORF 1a and nsp12–16 encoded in ORF1b (Ziebuhr et al., 2000). ORF 1a encodes three protease domains, one or two papain-like domains in nsp3 depending on the particular coronavirus, and one picornavirus 3C-like domain in nsp5 (Schiller et al., 1998; Weiss et al., 1994). Nsp8 in ORF 1a contains a second RNA-dependent RNA polymerase (RdRp) domain that is proposed to function as a primase and produce primers utilized by the primer-dependent nsp12 RdRp (Imbert et al., 2006). ORF 1b encodes an RNA-dependent RNA polymerase core unit in nsp12 (although a variable number of nts of the nsp12 coding sequence lies within ORF 1a, depending on the particular virus), a superfamily 1 helicase in nsp13, an exonuclease and N-methyltransferase in nsp14, an endoribonuclease in nsp15, and an S-adenosylmethionine-dependent 2′-*O*-methyl transferase in nsp16 (Bhardwaj et al., 2004; Chen et al., 2009; Cheng et al., 2005; Ivanov and Ziebuhr, 2004; Lee et al., 1991; Pinon et al., 1999; Putics et al., 2005; Snijder et al., 2003). The enzymatic activities of the exonuclease, endoribonuclease and S-adenosylmethionine-dependent 2′-O-methyl transferase encoded by nsp14, 15 and 16 are unique to Nidoviruses. Subgenomic mRNAs encode the major viral structural proteins including spike proteins (S), envelope protein (E), membrane protein (M), nucleocapsid protein (N), and the accessory proteins. Spike protein binds to the specific receptor on host cell plasma membranes. S is a class I fusion protein inducing cell fusion. In some betacoronaviruses and all gammacoronaviruses, the precursor polypeptide is cleaved by a cellular protease into noncovalently associated amino-terminal S1 and carboxy-terminal S2 subunits. The receptor binding domain (RBD) of MHV S1 determines receptor specificity, and S2 contains the transmembrane domain and two heptad repeat regions (HR1 and HR2) required for fusion activity (McRoy and Baric, 2008). On the other hand, the spike protein is uncleaved in most alphacoronaviruses and the betacoronavirus SARS-CoV. Both E and M are required for normal virion assembly in MHV (Fischer et al., 1998; Maeda et al., 2001), but E protein is not required for assembly for all coronaviruses (DeDiego et al., 2007; Kuo and Masters, 2003). Nucleocapsid protein binds to viral mRNA genome to form the ribonucleoprotein complex and also displays an RNA chaperone activity *in vitro* (Baric et al., 1988; Grossoehme et al., 2009; Masters, 2006; Nelson et al., 2000; Stohlman et al., 1988; Zuniga et al., 2007). This RNA chaperone activity has been proposed to have an important role in genome replication and sgRNA transcription (Zuniga et al., 2007). N proteins contain two structurally independently RNA binding domains, the N-terminal RNA binding domain (NTD) and a C-terminal domain (CTD, residues 256–385) which also has RNA binding activity, joined by a charged linker region rich in serine and arginine residues (SR linker) (Chang et al., 2009; Grossoehme et al., 2009). The NTD makes a specific and high affinity complex with the TRS or its complement (cTRS) and fully unwinds a TRS-cTRS duplex that plays a critical role in subgenomic RNA synthesis and other processes requiring RNA remodeling (Cologna et al., 2000; Grossoehme et al., 2009; Hurst et al., 2009; Zuniga et al., 2010). The N3 domain (residues 409–454) which extends to the true C-terminus of the N protein plays a role in determining N-membrane protein interaction in MHV (Hurst et al., 2005).

2.3. Viral RNA synthesis

Viral RNA synthesis occurs in the cytoplasm on double-walled membrane vesicles (Gosert et al., 2002; Knoops et al., 2008). During MHV RNA replication and transcription of subgenomic RNAs, the genomic RNA serves as a template for the synthesis of full-length and subgenomic negative-strand RNAs, the latter through a discontinuous transcription mechanism (Sawicki and Sawicki, 1990, 1998; Sola et al., 2005; van Marle et al., 1999; Zuniga et al., 2004). In turn, full-length negative-strand RNAs serve as templates for the synthesis of genome RNA and negative strand subgenomic RNAs serve as the templates for subgenomic mRNA synthesis. In this discontinuous transcription model, negative-strand subgenomic RNAs are transcribed from a genome-length template and leader-body joining is accomplished during the synthesis of negative-strand subgenomic RNAs through a copy-choice like mechanism involving TRS-B and TRS-L sequences (Pasternak et al., 2003; Sawicki and Sawicki, 1990, 1998; van Marle et al., 1999; Zuniga et al., 2004). In an elaboration of this model, viral and/or cellular factors binding to *cis*-acting RNA elements in the genomic RNA 5′ untranslated region (5′UTR) and 3′UTR, might circularize the genome, promoting template switching by topologically enabling base pairing between TRS-L and the nascent complementary TRS-Bs by the viral transcriptase/replicase complex (TRC) (Sola et al., 2005; Zuniga et al., 2004). Recently Mateos-Gomez et al. (2013) characterized a long-distance RNA–RNA interactions within the genomic RNA of TGEV, that serves as a transcriptional enhancer by bringing the TRS-L and TRS-B controlling N gene transcription into close proximity, raising the possibility that other similar long range RNA–RNA interactions might be present in other abundantly transcribed subgenomic RNAs.

3. 5′-*cis*-Acting RNA elements in coronavirus replication and transcription

The coronavirus RNA 5′UTR, the adjacent sequences encoding the amino-terminus of nonstructural protein1 (nsp1) and the 3′UTR contain *cis*-acting sequences that fold into secondary and higher-order structures, which contribute to their stability and to their involvement in inter- and intra-molecular interactions. Those structures are functionally important for RNA–RNA interactions and for the binding of viral and cellular proteins during RNA replication and translation (Brian and Baric, 2005; Liu and Leibowitz, 2010; Liu et al., 2009b) but cannot be complemented in *trans*. Many *cis*-acting sequences and their functional roles in viral transcription and replication were initially defined and studied in defective interfering (DI) RNAs (Chang et al., 1994; Dalton et al., 2001; Kim and Makino, 1995; Liu et al., 2001; Makino et al., 1985, 1988; Raman et al., 2003; Raman and Brian, 2005). These DI RNAs

are largely deleted but contain the *cis*-acting sequences necessary for their replication, including the 5′UTR and 3′UTR. DI RNAs replicate by using the RNA synthesis machinery of helper virus which provides replicase components in *trans*, and often interfere with viral genomic RNA replication. Several studies showed that approximately 400 nts to 800 nts at the 5′ end and 400 nts at the 3′ end of MHV RNA genome are necessary for DI RNA replication (Kim et al., 1993; Lin and Lai, 1993; Luytjes et al., 1996). The minimal length of 5′ sequence that supported MHV DI replication is 467 nts (Luytjes et al., 1996); the 3′UTR contains all the 3′ *cis*-acting sequences necessary for this process (de Haan et al., 2002; Goebel et al., 2004a). In BCoV the 5′ 498 nts act as a *cis*-acting signal for DI RNA replication (Chang et al., 1994). The development of reverse genetic systems for a number of coronaviruses has allowed the study of *cis*-acting sequences and their functions in the context of the whole viral genome.

MHV, BCoV and SARS-CoV are closely related in the Betacoronavirus genus (Gorbalenya et al., 2006). The secondary structures in the 5′-end-proximal genomic regions of these three viruses are largely conserved even though the nucleotide sequences are relatively divergent (Chen and Olsthoorn, 2010; Guan et al., 2012). A series of studies by consensus covariation modeling, chemical probing, SHAPE technology, and nuclear magnetic resonance (NMR) spectroscopy in conjunction with reverse genetics have been carried out, in order to characterize the predicted secondary structures of *cis*-acting sequences in the 5′UTR and the N-terminal nsp1 coding region of MHV and BCoV and to identify their functional roles in viral replication (Chen and Olsthoorn, 2010; Guan et al., 2011, 2012; Li et al., 2008; Liu et al., 2007, 2009a; Yang et al., 2011, 2015).

3.1. Secondary structure models

The 5′-most 140 nts of the MHV genome have been predicted to contain three conserved stem-loops (SL) 1, 2 and 4 based on a consensus secondary structural model from nine representative coronaviruses using phylogenetic analysis, ViennaRNA, Mfold and PKNOTS (Kang et al., 2006a; Liu et al., 2007). The nine coronaviruses modeled include five Beta-CoVs: BCoV, human coronavirus HCoV-OC43, HKU1, SARS-CoV, MHV-A59; three Alpha-CoVs: HCoV-NL63, HCoV-229E and TGEV; and one Gamma-CoV, IBV. The secondary structural models of the 5′ 140 nts of these coronaviruses are remarkably similar, and all contain three conserved helical stems, SL1, SL2, and SL4. SARS-CoV and BCoV are also predicted to contain an additional stem-loop, SL3, which folds the leader TRS (TRS-L) sequences into a hairpin loop. For MHV, a similar base pairing scheme for SL3 can be drawn (Chen and Olsthoorn, 2010), but the SL3 stem is not predicted to be stable at 37 °C (Liu et al., 2007). The secondary structures of the 5′UTR and adjacent coding sequences in all CoVs predicted by a structural-phylogenetic analysis (Chen and Olsthoorn, 2010) are largely consistent with the models by Kang et al. (2006a) and Liu et al. (2007).

In a recent study (Yang et al., 2015), SHAPE technology was utilized to determine the secondary structures formed by the 5′ most 474 nts *cis*-acting region required for replication of MHV-A59 DI RNA. The structure generated (Fig. 1A) was in excellent agreement with our previous characterization of SL1 (Li et al., 2008), SL2 (Liu et al., 2007, 2009a) and the correct structure for SL4 at position nts 80–130 (Yang et al., 2011). These stem-loops serve as *cis*-acting elements required for driving subgenomic RNA synthesis. Interestingly, the stem predicted for SL3 by phylogenetic algorithms (Chen and Olsthoorn, 2010) in the TRS region was single-stranded with relatively high SHAPE reactivity, consistent with the prediction of Liu et al. (2007) that this region was weakly paired or unpaired. The structure was also in good agreement with the two recent models of MHV-A59 RNA secondary structure (Guan et al., 2011, 2012) that identified two additional *cis*-acting replication elements required for optimal viral replication. S5 (Fig. 1), which contains a long-range RNA–RNA interaction (nts 141–167 base paired with nts 363–335) was equivalent to the base pairing (nts 141–170 paired with nts 363–332) predicted by Guan et al. (2012), with the exception of nts 332–334, which are unpaired in the Guan model but are part of the SL5C stem in the SHAPE-informed model (Fig. 1A). SL5A (nts 171–225) was identical to the stem-loop designated as SLIV previously (Brown et al., 2007; Guan et al., 2011). Furthermore, SL5A is remarkably similar to a stem-loop, predicted and designated SL5 by Chen and Olsthoorn (2010) based upon a structural-phylogenetic analysis of the 5′UTRs of betacoronaviruses. SHAPE analysis has also provided biochemical support for SL5B, SL5C, SL6 and SL7, which, in MHV, previously lacked support from genetic or biochemical studies.

Previously, the Brian lab defined four stem loops, SLI, II, III and IV, within the 210 nts 5′UTR of BCoV using the Mfold algorithm and their existence is supported by enzymatic probing and mutational analysis in DI RNA replication assays (Chang et al., 1994; Raman et al., 2003; Raman and Brian, 2005). It should be noted that the four stem loops defined by the Brian lab differ from the structures predicted by our group, except that SLIII in the Brian model is almost identical with the predicted SL4b in MHV (Kang et al., 2006a).

Fig. 1 shows a comparison of the secondary structure of MHV-A59 informed by SHAPE analysis (Fig. 1A) with the most thermodynamically stable models of the 5′ most 474 nts of BCoV-Mebus (Fig. 1B), SARS-CoV (Fig. 1D), and MERS-CoV (Fig. 1C), generated by RNAstructure software without incorporating any SHAPE reactivity data. In general, the overall configuration of the three models is similar despite the relatively high divergence of the nucleotide sequence. A core feature is a conserved SL5ABC four-helix junction, a finding strongly consistent with a conserved core architecture (Laing and Schlick, 2009). The initiation codon for nsp1 is in a similar position in SL5A in the two lineage A beta-CoVs, MHV and BCoV, whereas the initiation codon for SARS-CoV (lineage B) nsp1 and MERS-CoV (lineage C) are in more 3′ positions, in the first part of the 3′ side of S5 for SARS-CoV and in SL5B for MERS-CoV, as shown in Fig. 1. All four models contain the long-range base-pairing between 5′UTR sequences and the nsp1 coding region that make up the S5 stem. The lengths of connecting single-stranded junctions between the helices are also generally similar or identical, although the single stranded junctions between SL5A and the other two helices (S5 and SL5B, see Fig. 1) are shorter for BCoV than they are in MHV or SARS-CoV. The majority of the RNAstructure-based model for BCoV-Mebus (Fig. 1B) is in good agreement with the model for the 5′UTR and N-terminal nsp1 coding region of BCoV generated by Mfold modeling, phylogenetic covariation, and biochemical and genetic studies (Brown et al., 2007; Chen and Olsthoorn, 2010; Guan et al., 2011, 2012; Kang et al., 2006a; Liu et al., 2007; Raman et al., 2003; Raman and Brian, 2005), although the nomenclature is not equivalent. Parts of the RNAstructure-based model for SARS-CoV (Fig. 1D) are also similar to the model for the 5′ proximal sequence of SARS-CoV developed through structural-phylogenetic analysis, especially the presence of the substructures, SL5A, 5B and 5C which have been proposed to function in genome packaging (Chen and Olsthoorn, 2010). Following the S5 helical stem, the structures generated by RNAstructure are more divergent among the four viruses with MHV-A59 and BCoV-Mebus being relatively similar, although SL6 and SL7 are predicted to be in a forked stem-loop structure for BCoV whereas for MHV they form separate stem loops, and for SARS-CoV, three stem-loops, SL6, SL7 and SL8, are predicted. In MERS-CoV this region is predicted to fold into two bulged stem-loop structures, although their structure and position differs from that of MHV.

SHAPE analysis for *in vitro* transcribed and refolded RNA and *ex virio* genomic RNA in the 5′ *cis*-acting region generated identical secondary structures (Yang et al., 2015) and was generally

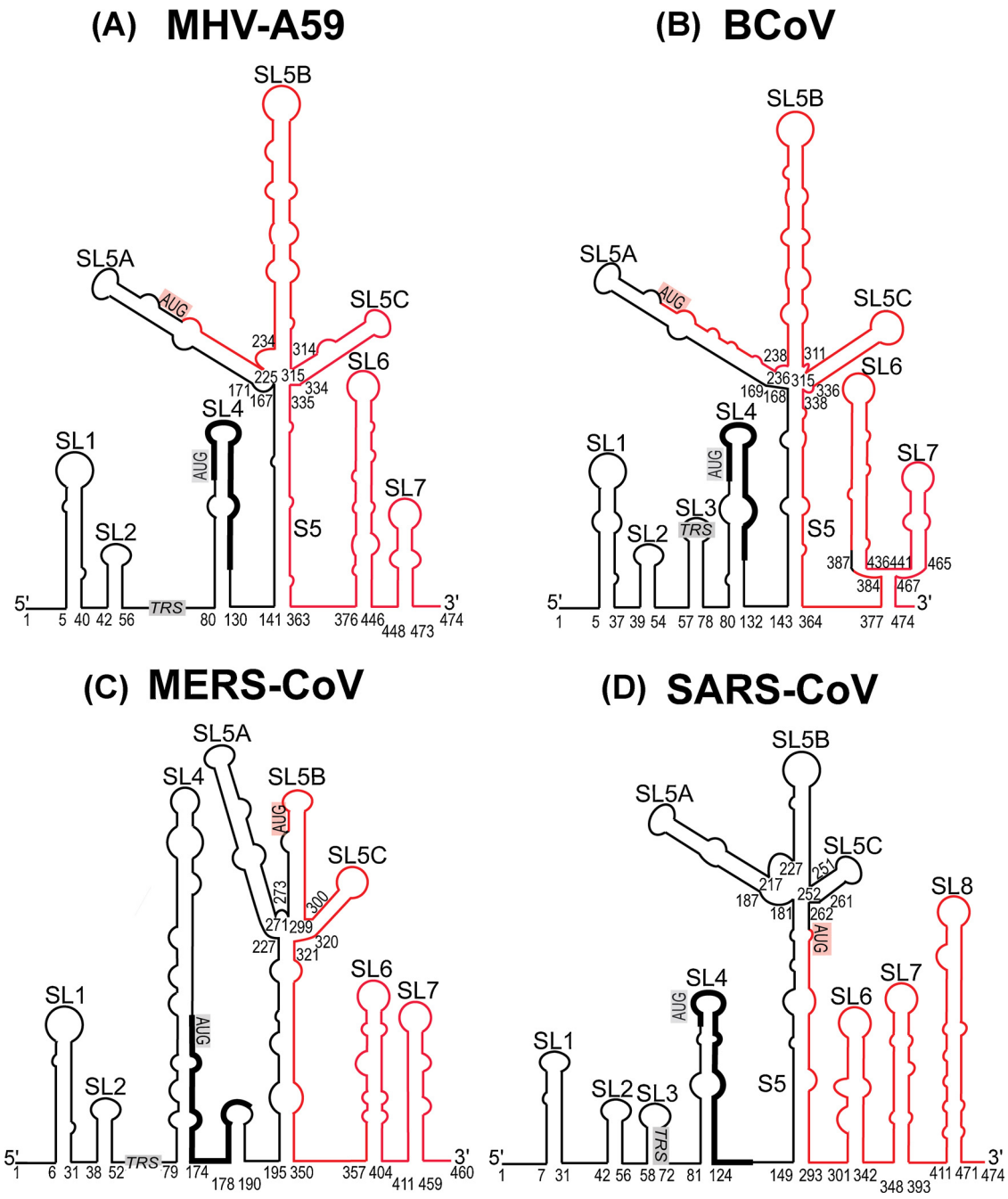

Fig. 1. Comparison of secondary structure models of the 5′ regions of MHV-A59, BCoV, MERS-CoV and SARS-CoV. (A) The MHV-A59 model was generated by SHAPE analysis. (B) The thermodynamically most stable models of the corresponding regions of BCoV-Mebus, (C) MERS-CoV (Al-Hasan 3), and SARS-CoV (D) were generated by RNAstructure. The gray and italicized text denotes the core leader TRS regions. The gray AUGs represent the start codons of the short open reading frames (heavy black lines) that are upstream from the nsp1 initiating AUG codons (pink shading) in all four viruses. The nsp1 open reading frames are indicated by the red lines. Note that the nomenclature for BCoV is not equivalent to that of previous studies by the Brian Laboratory (see text); SL1 and SL2 corresponds to SLI, SL3 to SLII, SL4 to SLIII, SL5A to SLIV, SL5B to SLV, SL5C to SLVI, S5 to a long-range RNA–RNA interaction, and SL6 to SLVIII.

consistent with previous studies of RNA secondary structure in this region. This gives us confidence that this methodology will be useful to explore the fine and long range secondary structures in the context of genomic RNA from authentic viral particles, particularly to determine the interactions of the intergenic regions and their flanking sequences which are likely to play a role in regulating template switching in MHV sgRNA synthesis.

The four betacoronavirus RNAstructure-based models described above share the conserved SL1, SL2, SL4 and SL5ABC secondary structure elements with the sequence covariation-based models of the CoV 5′UTR (Chen and Olsthoorn, 2010; Kang et al., 2006a; Liu et al., 2007). This conservation of SL1, SL2, SL4, and SL5ABC among the betacoronaviruses and SL1, SL2, and SL4 among alpha, beta, and gamma, coronaviruses suggests that these secondary structures serve as common *cis*-acting signals important in CoVs replication and viral RNA synthesis. Functional analyses of individual structural elements described below suggest that the structural features of SL1, SL2 and SL4 are more important than the precise nucleotide sequences in these stem-loops. However it should be noted that in BCoV and SARS-CoV SL3 overlaps TRS-L, which defines the leader-body junction region for discontinuous sgRNA synthesis, while SHAPE analysis indicates that the corresponding region is

single-stranded in MHV, consistent with the prediction of Liu et al. (2007). Thus for this region primary sequence is the functionally important feature.

3.2. Functional studies of individual structural elements

Although the RNA secondary structure of the 5′UTR of coronaviruses appears to be conserved across at least three genera, functional analyses of the individual stem-loop structures have only been performed on two betacoronaviruses, MHV and BCoV. The individual stem-loop structures contained in the 5′UTRs of related betacoronaviruses are largely interchangeable, with the exception of their TRSs (Kang et al., 2006a). The HCoV-OC43 SL1 can functionally replace the MHV SL1 (Li et al., 2008). SARS-CoV SL1, SL2, and SL4 can separately replace their corresponding MHV counterparts in the MHV genome, however, the MHV chimera is not viable when the entire MHV 5′UTR is replaced by the SARS-CoV 5′UTR even when the MHV leader TRS is substituted for the SARS TRS (Kang et al., 2006a). Replacement of each of four 5′ end *cis*-acting stem-loops, SL1, SL2, SL4 and SL5A in the MHV genome with their counterparts in the BCoV genome yields chimeric viruses with near-wild-type MHV phenotypes. However, the 32 nts (nts 142–173, see Fig. 1) which make up the 5′ side of S5 in the BCoV 5′UTR and which were predicted to be single-stranded in an earlier thermodynamic and phylogenetic model (Guan et al., 2011), cannot directly replace the equivalent sequences in MHV without genetic adaptation (Guan et al., 2011, 2012). These adaptations suggested that a long range interaction between nts 141–170 with nts 332–363 (S5, Fig. 1A) is required for optimal viral replication (Guan et al., 2012).

In addition, Fig. 1 shows the near identity of the location of the initiating AUG for MHV-A59 and BCoV-Mebus in SL5A, and the more 3′ location for the SARS-CoV initiation codon in the 3′ side of S5. An attempt to create an MHV chimeric virus in which the entire MHV 5′UTR was replaced by the SARS-CoV 5′UTR failed, even when the MHV leader TRS was substituted for the SARS-CoV TRS (Kang et al., 2006a). The likely explanation for this failure is the different locations for the initiating AUGs of the two viruses. Thus the replacement of the MHV 5′UTR with the SARS-CoV 5′UTR would disrupt the long-range interaction in S5. Similarly, the BCoV 32 nts region (nts 142–173) could not directly replace the corresponding 30 nts sequences in MHV-A59 without genetic adaptation (Guan et al., 2011), which is likely explained by partial disruption of base-pairing in S5, a long-range interaction between this region (nts 142–173) and sequences approximately 200 nts downstream within the nsp1 coding sequence in both MHV and BCoV.

A new member of the betacoronaviruses, MERS-CoV, is a close relative of bat coronaviruses HKU4 and HKU5 (Drexler et al., 2014). Prediction with RNAstructure (Mathews et al., 2004) showed that the most stable secondary structures in the 5′ end 350 nts region for MERS-CoV and Bat CoV HKU5-1 are very similar and are also similar to those for MHV, BCoV and SARS-CoV, containing conserved stem-loops SL1, SL2, SL4 and SL5ABC which contains a four-helix junction in the models for all four viruses (Fig. 1). One difference in the MERS-CoV predicted structure is the presence of a short stem-loop located at positions 178–190 between SL4 and SL5ABC that is unlabeled in Fig. 1C. The functional significance of this stem-loop remains to be investigated. Both MERS-CoV and Bat CoV HKU5-1 have single-stranded region between SL2 and SL4.

3.2.1. SL1

The MHV 5′UTR SL1 has been shown to be functionally and structurally bipartite by a detailed mutational and biophysical study (Li et al., 2008). Two pyrimidine–pyrimidine non-canonical base pairs divide the SL1 helical stem into upper and lower parts. The upper part of SL1 is required to be base-paired for efficient virus replication. Mutations that destroy base pairing of this region are lethal or generate viruses with impaired phenotypes. Compensatory mutations introduced in both sides of the stem that restored the base pairing produce viable viruses with phenotypes similar to wild type virus. In contrast, the viruses containing mutations that destroy base pairing in the lower region of SL1 are viable, and the compensatory mutations predicted to restore base pairing are lethal, suggesting that the sequences rather than base pairing in the lower portion of the SL1 stem are required. Genomes carrying lethal mutations in SL1, fail to direct the synthesis of minus-sense subgenomic RNA implying that this element has a crucial role in this process, possibly related to template switching events during leader-body joining (Li et al., 2008). Deletion of a bulged A35 in the lower portion of the stem increases the thermal stability of the helix. Recovered viruses all contained destabilizing second-site mutations near the A35 deletion, suggesting that structural lability of the lower region of SL1 is important for virus replication. The recovered viruses also contain additional mutations, A29G or A78G in the 3′UTR, providing genetic evidence supporting an interaction between the 5′ and 3′UTRs, as hypothesized in one model of coronavirus subgenomic mRNA synthesis (Zuniga et al., 2004). A dynamic SL1 model is proposed in which the base of SL1 has an optimized lability required to mediate a physical interaction between the 5′UTR and the 3′UTR that stimulates subgenomic RNA synthesis (Li et al., 2008).

3.2.2. SL2

SL2 is the most conserved secondary structure in the coronavirus 5′UTR, with a 5 nt long stem capped with a (C/U)UUG(U/C) pentaloop being the single most conserved sequence in the 5′UTR (Liu et al., 2007). Replacing U48 with C or A is lethal, but the virus containing a U48G mutation is viable and grows with nearly a WT phenotype. Initial NMR studies of SL2 suggested that the imino proton of U48 in the WT sequence or G48 in a U48G mutant donates a hydrogen bond suggesting that it might stabilize a U-turn like conformation, which is consistent with the genetic results (Liu et al., 2007). However, further NMR study showed that MHV SL2 takes on a structure incompatible with a canonical U48-U49-G50 U-turn loop structure, but better fits with an uYNMG(U)a-like or uCUYG(U)a-like tetraloop structure with U51 flipped out and G50 stacked on A52 (Liu et al., 2009a). Furthermore, the structure of the SARS-CoV SL2 has been determined at atomic resolution showing that the SL2 pentaloop is stacked on 5-bp stem and adopts a canonical CUYG tetraloop fold with U51 flipped out of the stack (Lee et al., 2011), making it likely that MHV SL2 has a similar structure. Further mutational studies of the loop demonstrate that any nucleotide replacement at C47, U49 and U51 can function and produce viable mutant viruses, whereas the G at position 50 is required (Liu et al., 2007, 2009a). Mutational analysis of the SL2 stem demonstrates that the stem is required for viral viability whereas its nucleotide sequences are not important. RT-PCR analyses of the genomes containing lethal mutations in SL2 indicate that SL2 is required for subgenomic RNA synthesis (Liu et al., 2007).

3.2.3. TRS

The TRS regions of some coronaviruses, SARS-CoV and BCoV for example, are predicted to fold the leader TRS sequences into a hairpin loop, designated SL3. For the related betacoronavirus MHV, a similar base pairing scheme for SL3 can be drawn (Chen and Olsthoorn, 2010), but the SL3 stem is not predicted to be stable at 37 °C (Liu et al., 2007). Structural probing of MHV suggests that the TRS region is single stranded (Yang et al., 2015). The leader TRS has a key role in subgenomic mRNA synthesis. The discovery and cloning of DI RNAs enabled a series of experiments using *in vitro* transcribed DI RNAs containing a reporter gene under the control of either mutant and wild type TRS sequences to probe the sequence

requirements for leader-body joining during subgenomic RNA synthesis (Hiscox et al., 1995; Makino et al., 1991; van der Most et al., 1994). These experiments demonstrated that there is a requirement for a minimum degree of sequence similarity between the TRS-L and TRS-B for transcription to proceed. However the relationship between the level of sequence similarity between TRS-L and TRS-B and the transcriptional activity at a TRS was not entirely straight-forward and thus additional factors are thought to play a role. In two elegant mutational studies employing a TGEV reverse genetic system this question was re-investigated in the context of infectious virus (Sola et al., 2005; Zuniga et al., 2004). Extending the region of potential base pairing between TRS-L and the complement of TRS-B to include 4 nts of TRS 5′ and 3′ flanking sequence allowed Sola et al. to predict the ability of each TRS sequence to promote transcription based on the Gibbs free energy of the base pairing of this region (Sola et al., 2005).

3.2.4. SL4

Previously, the Brian lab showed a BCoV stem-loop they designated as SLIII mapping at nts 97 through 116 in the BCoV 5′UTR, which must be base-paired for BCoV DI RNA replication (Raman et al., 2003). Later Chen and Olsthoorn (Chen and Olsthoorn, 2010) employed a phylogenetic approach to predict the existence of SL4 downstream of the TRS-L, nts 80 through 130 in MHV, which differs primarily from SL4 in the model predicted by Leibowitz/Giedroc group in that the proximal 6 nts at left side (nts 74–79) and right side (nts 139–134) of SL4 are base paired (Kang et al., 2006a; Liu et al., 2007). For MHV, SL4 was predicted by the Leibowitz/Giedroc group (Kang et al., 2006a; Liu et al., 2007) to be positioned just 3′ to the leader TRS and is the first proposed structural RNA element of the 5′UTR 3′ of the leader (Fig. 1A). It is predicted to contain a bipartite stem-loop, SL4a and SL4b, separated by a bulge (Kang et al., 2006a; Liu et al., 2007). SL4b in this model corresponds to SLIII in BCoV 5′UTR (Raman et al., 2003).

Mutations that disrupt the helix in the SLIII in BCoV 5′UTR (Raman et al., 2003) led to loss of RNA accumulation of mutant DI RNA, whereas compensatory mutations that restore the structure result in some level of RNA accumulation of double mutant DI RNA progeny. The Brian group also tested the functional role in viral replication of a short AUG-initiated intra-5′UTR ORF (this is represented by the heavy line in Fig. 1) that is present in BCoV, potentially encoding an eight-amino-acid peptide which is phylogenetically conserved, especially among betacoronaviruses. They reported that the amino acid sequences of the intra-5′UTR ORF are important for BCoV DI RNA accumulation and there is a positive correlation between the maintenance of the short ORF and maximal DI RNA accumulation (Raman et al., 2003). The MHV 5′UTR also contains an eight-amino-acid small ORF in SL4b, identical to that present in the corresponding region of BCoV (Raman et al., 2003). Yang et al. (2011) performed an extensive mutational analysis of MHV SL4, and as part of that study demonstrated that the eight amino acid small ORF did not have a critical role in MHV replication. This is contrary to the finding in BCoV DI RNA replication assays that these elements are necessary to continually passage BCoV DI RNA (Raman et al., 2003; Raman and Brian, 2005), but is consistent with a later study by the Brian group which demonstrated that there is positive selection for the small upstream ORF, but it is not essential for MHV replication in cell culture (Wu et al., 2014). The likely explanation for the conflicting results from DI assays and assays done with similar mutants in the context of a complete viral genome is that by their very nature DI replication assays are competition assays with helper wild type virus and recombinant WT DI RNAs that arise during the experiment. Thus the DI experiments may have detected subtle decreases in relative fitness in the BCoV DI RNA replication that are not detected in straight forward viral replication assays that focus on recovering viable viruses. The mutational study of SL4 by Yang et al. (2011) also indicates that for SL4b, neither the structure nor the sequence have a critical role in viral replication. The parallel analysis of SL4a was consistent with the Chen phylogenetic based model of SL4 (Chen and Olsthoorn, 2010) leaving nts 74–79 and 131–139 unpaired. However, deletion of the entire MHV 5′UTR SL4 is lethal and the genome carrying this deletion is defective in directing subgenomic RNA synthesis. A viable mutant in which SL4 was replaced with a sequence unrelated stem-loop supports the hypothesis that SL4 functions in part as a “spacer element” and this spacer function plays an important role in directing subgenomic RNA synthesis during virus replication (Yang et al., 2011).

3.2.5. SL5

The Brian group determined that a stem loop that they designated SLIV (corresponding to SL5A in Fig. 1) spanning nts 171–225 and thus extending into the nsp1 coding sequence was required for optimal replication of MHV (Guan et al., 2011). Nucleotides 238–262 and nts 284–309 make up a segment of the bulged stem-loop designated SL5B in a SHAPE-generated model (Fig. 1), and correspond to an identical stem-loop structure that was predicted as the basal segment of SLV (nts 238–262 and nts 284–309) for betacoronavirus by Mfold and by covariation analysis (Brown et al., 2007), and as part of an unnamed stem-loop by a structural-phylogenetic analysis of betacoronavirus (Chen and Olsthoorn, 2010). The SHAPE-generated model differs from earlier models in that nts 234–237 are base-paired with nts 314–310 in the base of SL5B but these nucleotides are not included in SLV (Brown et al., 2007) or the corresponding region in Chen model (Chen and Olsthoorn, 2010). Moreover, the structure predicted by SHAPE analysis for nts 263–283 in the terminal part of SL5B agrees with that predicted by the Chen model (Chen and Olsthoorn, 2010), but is different from the stem-loop predicted for the terminal portion of BCoV SLV by Brown et al. (2007). BCoV SLV (nts 239–310) is also supported by RNase structure probing (Brown et al., 2007). SL5C (nts 315–334) is similar to the distal part of SLVI predicted by Brown et al. (2007) and to the corresponding region in the Chen model (Chen and Olsthoorn, 2010). BCoV SLVI has been identified as a *cis*-acting element required for DI RNA replication (Brown et al., 2007). In a recent study (Yang et al., 2015), disruption of SL5C by four nucleotide substitutions while maintaining the WT amino acid sequence resulted in viable recombinant viruses with only moderate impairment of virus replication compared to that of the WT virus, suggesting that the *cis*-acting SL5C is not required for viral replication. This contrasts to the data obtained with a BCoV DI RNA model replicon, where the destruction of the distal helix that corresponds to SL5C resulted in a failure of DI RNA replication (Brown et al., 2007). We have previously found similar discordant results with MHV DI RNAs and recombinant viruses containing identical mutations in their 3′UTRs (Johnson et al., 2005), and subsequently with recombinant MHVs containing SL4b mutations (Yang et al., 2011) when compared with a BCoV DI RNA containing similar mutations (Raman et al., 2003). Currently we reason that the nature of DI replication assays, in which a mutant DI RNA must compete with helper wild type virus and recombinant WT DI RNAs that arise during the experiment, allow DI replication experiments to magnify modest decreases in fitness observed in straight forward viral replication assays that focus on recovering viable viruses, making them much more severe or lethal in DI RNA replication assays.

3.2.6. SL6-7

SL6 spans nts 376–446 in MHV-A59 and encodes nsp1 amino acid positions 56–79. The SHAPE-generated SL6 (nts 376–446) (Fig. 1) is remarkably similar to SLVIII, predicted by Mfold for betacoronavirus (Brown et al., 2007), but no structural or functional evidence supported the SLVIII prediction. A mutational study (Yang et al., 2015) demonstrates that MHV SL6 is not essential for viral

replication. In a previous study by Brockway and Denison (2005) a genome (designated VUSB5) containing nsp1 charge-to-alanine mutations in the base of the SL6 helix, nts 399–401, CGG → GCA (R64A), and at nts 414–416 GAA → GCA (E69A), was not viable. These mutations are predicted to destabilize the distal stem of SL6. A second mutation, VUSB6, includes substitutions at nts 441–446, CGUGAU → GCAGCA (R78A, D79A), was also not viable. Because the RNA secondary structure in these putative *cis*-acting regions was not known at the time, Brockway and Denison (2005) could not unequivocally assign the functional effects of these mutations on replication to the amino acid alterations in nsp1. Modeling the effects of these mutations on the secondary structure of SL6, indicates that VUSB5 would destabilize the distal portion of SL6 and VUSB6 is predicted to completely open up the bottom of SL6. In light of the viability of the mutations that destabilize the distal region of SL6 (SL6-B) (Yang et al., 2015), and the ability of Brockway and Denison (2005) to recover viable viruses containing mutations (VUSB4) in nsp1 that are predicted to destabilize the base of SL6 very much as did the lethal VUSB5, it is very likely that the lethality of VUSB5 and VUSB6 are due to their effects on nsp1 rather than due to effects on RNA secondary structure.

SL6 and SL7 in MHV-A59 diverge somewhat from the corresponding structures in BCoV-Mebus, and are quite different from SL6-8 in SARS-CoV and SL6 and SL7 in MERS-CoV (Fig. 1). This is consistent with functional studies of SL6 which demonstrate that SL6 is not essential for MHV replication (Yang et al., 2015), in contrast to structural elements that are entirely within the 5′UTR (SL1, SL2, SL4) or to the trifurcated SL5 stem-loop which extends from the 5′UTR into the nsp1 coding sequence, which are lethal or result in viruses that are crippled for viral replication (Guan et al., 2011, 2012; Li et al., 2008; Liu et al., 2007, 2009a; Yang et al., 2011).

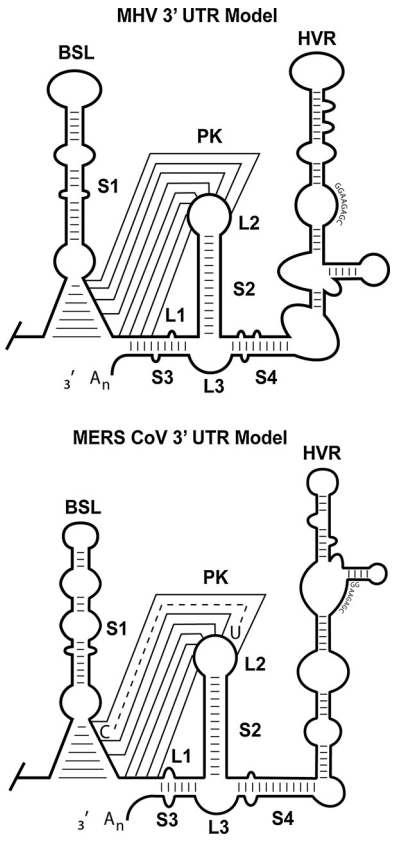

Fig. 2. A schematic drawing of the secondary structures of the 3′ untranslated regions of MHV and MERS-CoV. For the MERS-CoV the dotted line in the pseudoknot (PK) represent a potential non-canonical UC base pair.

4. 3′-*cis*-Acting RNA elements in coronavirus replication and transcription

The coronavirus 3′UTR consists of 300–500 nts plus a poly(A) tail, depending upon the particular coronavirus examined. Initial replication assays with MHV DI RNAs indicated that the minimal length of 3′ sequence required for MHV DI RNA replication was 436 nts, including part of the N gene and the entire 3′UTR 301 nts (Lin and Lai, 1993; Luytjes et al., 1996). The minimal sequences that support TGEV and IBV DI RNA replication are 492 nts and 338 nts, respectively, neither region includes any part of the N gene (Dalton et al., 2001; Mendez et al., 1996) and the presence of an accessory gene 3′ of the N gene in the alphacoronaviruses suggested that at least for these coronavirus genera the 3′UTR contains all of the signals needed for replication. Subsequent experiments in which the MHV N gene was separated from the 3′UTR in recombinant MHVs suggested that the 3′UTR contained all of the *cis*-acting sequences needed for replication in betacoronaviruses as well (de Haan et al., 2002). In a DI replication assay the minimal *cis*-acting signal essential for negative-strand RNA synthesis was only the 3′ most 55 nts of the genome plus the poly(A) tail (Lin et al., 1994). The poly(A) tail has been identified as an important *cis*-acting signal required for BCoV DI RNA replication, although as little as five As sufficed to initiate replication (Spagnolo and Hogue, 2000). The poly(A) tail has also been shown to be necessary for MHV minus-strand RNA synthesis (Lin et al., 1994).

A series of studies utilizing RNA folding algorithms, biochemical studies, and functional studies have been used to investigate the structure and function of various *cis*-acting elements present in the 3′UTR (Goebel et al., 2004a, 2007; Hsue et al., 2000; Hsue and Masters, 1997; Liu et al., 2001, 2013; Stammler et al., 2011; Williams et al., 1999; Zust et al., 2008) and the current best model of the 3′UTR is shown in Fig. 2 (Zust et al., 2008). The 5′-most secondary structure is a 68 nts bulged stem-loop just downstream of the N gene stop codon, and it is essential for MHV DI RNA and viral replication (Hsue et al., 2000; Hsue and Masters, 1997). This bulged stem-loop is predicted to be conserved among the betacoronaviruses and the pairing, but not the primary sequence, of the four covariant base pairs, is critical for the function of the secondary structure (Goebel et al., 2004b; Hsue and Masters, 1997). 3′ to the 68 nts bulged stem-loop is a hairpin stem-loop which can form a 54 nts hairpin-type pseudoknot, which is required for BCoV DI RNA replication (Williams et al., 1999). The pseudoknot is phylogenetically conserved among coronaviruses, both in location and in shape but only partially in nucleotide sequence, indicating that it may function as a regulatory control element. Computer assisted inspection of the MERS-CoV sequence indicated it is present in this newly recognized betacoronavirus as well, although in this virus the pseudoknot may contain a non-canonical base pair (Fig. 2). Goebel et al. (2004a) demonstrated that in MHV and BCoV, the bulged stem-loop and pseudoknot are in part mutually exclusive structures because they partially overlap and cannot be formed simultaneously (see Fig. 2). The authors proposed that the bulged stem-loop and pseudoknot are the components of a molecular switch which has the potential to regulate a transition occurring during viral RNA synthesis, and supported this hypothesis by a series of reverse genetic experiments (Goebel et al., 2004a).

Computer assisted modeling and biochemical probing of the RNA secondary structure of the last 166 nts of MHV downstream of the pseudoknot predicted a long multi-branch stem loop in this region of the genome (Liu et al., 2001). DI replication assays suggested that several of the stems in this region were functionally important. Paul Masters' group subsequently employed a reverse genetic approach and showed that for MHV the long hypervariable

bulged stem-loop structure between nts 46–156 is not essential for viral replication, even though it contains an octanucleotide sequence, 5′-GGAAGAGC-3′, which is highly conserved in the 3′UTR of coronaviruses (Goebel et al., 2007). Based on a reverse genetic study combined with a phylogenetic comparison of the 3′UTRs of a number of coronaviruses Zust et al. (2008) developed an improved model for the 3′UTR which is shown in Fig. 2. This model contains a triple helix junction in which stems designated S3 and S4 flank the hairpin stem-loop (S2-L2 in Fig. 2) which participates in the pseudoknot. Stammler et al. (2011) performed a series of biophysical studies demonstrating that the pseudoknotted conformation is much less stable than the double-hairpin conformation, but suggest that stacking of the pseudoknot with the S3 helix can stabilize the pseudoknotted conformation allowing it to form. Consistent with the biophysical studies, a reverse genetic study of this three helix junction region suggested that S3 is essential for viral replication (Liu et al., 2013). However, mutations disrupting the S4 helix of the triple helix junction, or deleting most of the L3 loop are tolerated.

For the alphacoronaviruses, although the pseudoknot is conserved the bulged stem loop (BSL in Fig. 2) that is 5′ to the pseudoknot is absent (Dye and Siddell, 2005). In the gammacoronaviruses a stem-loop located at the upstream end of the 3′UTR is required for viral replication (Dalton et al., 2001). Although a nearby pseudoknot is present in gammacoronavirus, its functional importance has not been established (Williams et al., 1999). Only in the betacoronaviruses are both the pseudoknot and the bulged stem-loop closely overlapped. Although the primary sequences diverge among the betacoronaviruses, the secondary structures are highly conserved and functionally equivalent (Goebel et al., 2004b; Hsue and Masters, 1997; Wu et al., 2003). MHV and BCoV 3′UTRs are interchangeable although the nucleotide sequences diverge by 31% (Hsue and Masters, 1997), and the SARS-CoV 3′UTR can replace its MHV counterpart without affecting viral viability (Goebel et al., 2004b; Kang et al., 2006b). However, the viable chimeras could not be recovered when the MHV 3′UTR was replaced with either the TGEV 3′UTR or the IBV 3′UTR (Goebel et al., 2004b; Hsue and Masters, 1997; Kang et al., 2006b).

5. Viral and cellular proteins binding to the 5′ and/or 3′ *cis*-acting RNA elements

In the negative-strand discontinuous RNA synthesis model proposed by Zuniga et al. (2004), viral and/or cellular factors binding to *cis*-acting RNA elements in the genomic RNA 5′UTR, TRS-L and 3′UTR, might circularize the genome through RNA–RNA, or RNA–protein and protein–protein interactions, and thus produce a topology enabling base pairing between TRS-L and the nascent complementary TRS-Bs during synthesis of minus strand RNA. A fair number of host proteins have been reported to interact with these *cis*-acting signals and these are reviewed below. It should be noted that majority of this work has been performed with MHV and although it is likely that functionally important host proteins and the elements that they recognize are likely to be conserved, it is possible that there might be some differences among the four coronavirus genera.

Two viral proteins have been shown to bind to the coronavirus 5′UTR, the N protein and nsp1 (Table 1). The MHV N protein binds with high affinity and specificity to the TRS-L and possesses helix unwinding properties that suggest a role in template switching (Baric et al., 1988; Grossoehme et al., 2009; Keane et al., 2012; Nelson et al., 2000), consistent with the demonstration that the TGEV and SARS N proteins have RNA chaperone activity (Zuniga et al., 2007). It has also been suggested that N protein binding to TRS-L favors translation of viral RNAs (Tahara et al., 1998). The N binding site in the leader RNA sequence in MHV is specifically localized to nts 56–72 (UAAAUCUAAUCUAAACU), and this interaction plays an important role in the discontinuous RNA transcription unique to Nidoviruses (Baric et al., 1988; Grossoehme et al., 2009; Keane et al., 2012; Nelson et al., 2000; Stohlman et al., 1988). N protein contains two structurally independent RNA-binding domains: an N-terminal RNA binding domain (NTD) and a C-terminal dimerization domain (CTD) (Hurst et al., 2010) linked by a Ser/Arg (SR)-rich linker. The N-terminal domain (NTD) of the CoV N protein functions as an RNA chaperone *in vitro* (Zuniga et al., 2007), binds to the TRS, and the NTD–TRS interaction is critical for efficient sgRNA synthesis in MHV (Grossoehme et al., 2009; Keane et al., 2012). The MHV NTD forms a high affinity ($K_{obs} \approx 8 \times 10^7\ M^{-1}$) 1:1 complex with a TRS-containing RNA (5′-gAAUCUAAAC) and its complement (cTRS) (Grossoehme et al., 2009). A recent study showed that the NTD–TRS interaction involves N residues R125, Y127, and Y190 and anchors the adenosine-rich region in the 3′ end of the TRS RNA to the β-platform of N and that this interaction is critical for efficient sgRNA synthesis (Keane et al., 2012). This same study also showed that the IBV and SARS-CoV N protein NTD shows limited binding specificity for their cognate TRS sequences (Keane et al., 2012). Thus it is not clear that the specific binding of N protein to the TRS over and above its general RNA binding activity plays a role in sgRNA synthesis for all coronaviruses. The second viral protein that has been shown to bind to the 5′UTR is nsp1 (Gustin et al., 2009). The BCoV nsp1 protein has been determined to bind to three *cis*-acting stem loops in the 5′UTR, including SLIII, which corresponds to SL4b in our model and to regulate viral RNA translation and replication (Gustin et al., 2009). It is likely that the closely related MHV nsp1 protein has a similar function.

A number of host proteins have been shown to bind to the 5′UTR as well (Table 1). The pyrimidine tract-binding protein (PTB) has been reported to bind to the pentanucleotide repeat UCUAA in the positive-strand MHV RNA leader TRS and a role in subgenomic mRNA synthesis was suggested based on a correlation between binding efficiency to different DI RNA constructs and the expression of a reporter under the control of a body TRS (Choi et al., 2002; Li et al., 1999). For TGEV PTB was also identified as binding to the genomic 5′UTR using an RNA affinity-mass spectroscopy approach (Galan et al., 2009). Heterogeneous nuclear ribonucleoprotein A1 (hnRNP A1) binds to the complement of the 5′ leader sequence (negative-strand leader) and to the complement of the TRS-B sequences (Choi et al., 2002; Li et al., 1997, 1999). The functional importance of this binding has been controversial, Shen and Masters (2001) tested the role of hnRNP A1 in MHV replication by investigating the ability of MHV to replicate in cells lacking a functional hnRNP A1. The infected cells supported viral replication and synthesized normal levels of genome and subgenomic RNAs, suggesting that hnRNP A1 is not required for MHV discontinuous transcription or genome replication. However, it has been shown that multiple other type hnRNPs, including hnRNP A2/B1, hnRNP A/B, and hnRNP A3, bind to the negative strand complement of the MHV leader TRS (Shi et al., 2003) and that overexpression of hnRNP A/B resulted in a 4–5 fold enhancement of viral RNA synthesis, suggesting that these proteins might also facilitate RNA synthesis and be able to substitute for hnRNP A1. Another member of the hnRNP family, synaptotagmin-binding cytoplasmic RNA-interacting protein (SYNCRIP), similarly binds to the MHV 5′UTR and to its negative strand complement (Choi et al., 2004). The L-TRS sequence has been shown to be necessary but sufficient for SYNCRIP binding and siRNA knockdown of SYNCRIP delayed the time of peak viral RNA synthesis in MHV infected cells (Choi et al., 2004).

Similarly to the 5′UTR, multiple proteins have been demonstrated to bind to the 3′UTR. A reverse genetic study by Zust et al. (2008) revealed that a 6 nt insertion between the 3′UTR pseudoknot and the S3 helix (see Fig. 2) crippled MHV replication but they identified second site mutations in nsp8 and nsp9 which restored viral

Table 1
Host and viral proteins that bind to 5′ and 3′ *cis*-acting regions.

Proteins bound	Viruses	Binding locations in virus genome 5′ end	Binding locations in virus genome 3′ end
Viral proteins			
N	MHV	5′UTR TRS-L in (+)RNA, specifically to nts 56–72 (UAAAUCUAAUCUAAACU)	
	TGEV, SARS-CoV	Specificity not determined, functions as RNA chaperone	
Nsp1	BCoV	5′UTR in (+)RNA, specifically to SLIII and its flanking sequences	
Nsps 8 and 9	MHV		Interaction with the 3′UTR in (+)RNA established genetically, binds specifically to the double hairpin adjacent to S3
Host proteins			
PTB	MHV	5′UTR TRS-L in (+)RNA, specifically to pentanucleotide repeat UCUAA	3′UTR in (-)RNA, specifically to nts 53–149*
	TGEV	5′UTR in (+)RNA	
hnRNP A1	MHV	5′UTR TRS-L and TRS-B in (-)RNA	3′UTR in (+)RNA
SYNCRIP	MHV	5′UTR in both strands	
hnRNPs (A2/B1, A/B, A3)	MHV	TRS-L in (-)RNA	
hnRNPs (A1, A0, A2/B1, Q, U); PABP; p100 transcriptional co-activator protein; arginyl-tRNA synthetase; EPRS	TGEV		3′ end of genome in (+)RNA
Mitochondrial aconitase, HSP70, HSP60, HSP40	MHV		3′ most 42 nts in (+)RNA, specifically to 11 nts UGAAUGAAGUU at position 26–36* and to 38 nts at 129–166*

replication to near normal levels. Based on this genetic result they suggested a model in which a complex of the nsp8 primase plus the associated proteins nsps 7, 9, and 10 binds to the double hairpin conformation of the 3′UTR just adjacent to S3 to initiate minus strand RNA synthesis. The nascent newly synthesized minus strand RNA would displace the 3′ half of the S3 helix and permit the formation of the RNA pseudoknot, also allowing binding of the main replicase complex containing nsp12, the main coronavirus RdRP, nsp13 (helicase), plus the associated RNA modification enzymes nsp 14–16 (Bhardwaj et al., 2004; Decroly et al., 2008; Ivanov and Ziebuhr, 2004; Minskaia et al., 2006; Snijder et al., 2003).

A number of host proteins have been reported to interact with the 3′UTR. Yu and Leibowitz reported four host proteins binding to the MHV 3′-most 42 nts RNA probes using RNase protection/gel mobility shift and UV cross-linking assays and a conserved 11 nts UGAAUGAAGUU sequence spanning position 26–36 in the 3′UTR (note that in this numbering system position 1 is the first nt upstream of the poly(A) tail) was necessary for protein binding activity and for efficient DI RNA replication (Yu and Leibowitz, 1995a,b). A second protein binding region was similarly mapped within a 38 nucleotide (nt) sequence 166–129 nucleotides upstream of the 3′ end of the MHV genome and was also found to be necessary for efficient DI RNA replication (Liu et al., 1997). Subsequent studies determined that the proteins binding to the MHV 3′-most 42 nts element include mitochondrial aconitase and the chaperones mitochondrial HSP70, HSP60 and HSP40 (Nanda et al., 2004; Nanda and Leibowitz, 2001). PTB has been shown to bind to a negative-strand RNA complementary to the MHV 3′UTR at position 53–149 and less strongly at positions 270–307 (Huang and Lai, 1999). Deletions in the 53–149 binding site that abolished PTB binding also strongly inhibited subgenomic mRNA synthesis in an MHV DI construct containing a reporter gene under the control of a TRS sequence (Huang and Lai, 1999). In addition to binding to the 5′UTR, hnRNP A1 has two binding sites in the MHV 3′UTR and these binding sites are complementary to the PTB binding sites in the negative sense 3′UTR enumerated above (Huang and Lai, 2001). DI RNAs containing a mutated hnRNP A1-binding site had reduced RNA transcription and replication activities. Using an RNA affinity–mass spectroscopy approach Galan et al. (2009) identified nine host proteins, including several hnRNPs (A1, A0, A2B1, Q, and U), the glutamyl-prolyl-tRNA synthetase (EPRS), arginyl-tRNA synthetase, poly(A) binding protein (PABP), and the p100 transcriptional co-activator that bound to the TGEV 3′UTR. A possible role for these proteins in TGEV replication was suggested by the siRNA-mediated knockdown of PABP, hnRNP Q and EPRS expression with a concomitant 2–3-fold decrease in TGEV RNA synthesis and viral titer in infected cells. Spagnolo and Hogue (2000) demonstrated an interaction of PABP with the poly(A) tail is required for BCoV and MHV DI RNA replication, and a tail length of 5 is sufficient to support DI replication.

6. Interactions between 5′ and 3′ ends and TRS

The widely accepted model of coronavirus discontinuous transcription of subgenomic RNA postulates that leader body joining occurs during the synthesis of minus strand RNAs (Baric and Yount, 2000; Sawicki and Sawicki, 1990; Sethna et al., 1989). Zuniga et al. (2004) have provided strong support for this model by showing that in TGEV the body TRS sequences upstream of each gene signal template switching to the TRS 5′ leader (TRS-L) and proposed a refinement of the model in which the 3′ and 5′UTRs interact through RNA–RNA and/or RNA–protein plus protein–protein interactions to promote circulization of the coronavirus genome to place the elongating minus strand in a favorable topology for leader-body joining.

Several candidate RNA–protein interactions have been identified and proposed to contribute to circulization of the genome. Spagnolo and Hogue (2000) suggested that the interaction of PABP bound to the coronavirus 3′ poly(A) tail might result in the circularization of the coronavirus genome through its ability to interact with eIF-4G, a component of the three-subunit eIF-4F cap binding protein that binds to mRNA cap structures during translation (Sonenberg, 1996; Sonenberg et al., 1978). An interaction between PTB bound to leader (and body) TRS has also been postulated to play a role in coronavirus transcription by mediating an interaction between the TRS and the 3′UTR by binding to hnRNP A 1 bound to its protein binding sites in the 3′UTR (Lai, 1997, 1998). Although this is an attractive model, the fact that a deletion encompassing the high affinity hnRNP A1 binding site in the 3′UTR is able to replicate and direct normal synthesis of subgenomic mRNAs makes the PTB-hnRNP A1 association less likely to have a crucial role in leader-body rejoining (Goebel et al., 2007), although the possibility that

other members of the hnRNP family could substitute for hnRNP A1 remains a possibility (see Section 5 for a discussion of this). Li et al. (2008) reported that viruses recovered after deletion of a bulged A35 in the lower portion of the 5′UTR SL1 stem contain additional second site mutations, A29G or A78G in the 3′UTR, providing genetic evidence in support of an interaction between the 5′ and 3′UTRs. They proposed a dynamic SL1 model in which the base of SL1 has an optimized lability required to mediate a physical interaction between the 5′UTR and the 3′UTR that stimulates subgenomic RNA synthesis. In unpublished work P. Liu and Leibowitz identified a potential base pairing between nucleotides 8–24 in the MHV 5′UTR SL1 and two discontinuous sequences in the 3′UTR, nts 1–6 and 218–228 (note that the 3′UTR sequences are numbered with position 1 corresponding to the first nucleotide 5′ of the poly (A) tail). An extensive mutational analysis of these sequences failed to provide genetic support for a functional role for this potential 5′–3′UTR interaction in MHV replication. Thus the precise mechanism by which the 5′ and 3′UTRs associate during viral replication remains to be functionally defined.

7. Conclusion and future directions

A series of studies utilizing consensus covariation modeling, chemical probing, nuclear magnetic resonance (NMR) spectroscopy, and SHAPE analysis have identified and characterized individual or small numbers of RNA secondary structures in the *cis*-acting region containing the MHV 5′UTR and extending into the N-terminal nsp1 coding sequence, TRS, 3′UTR and poly(A) tail and many of the studies have examined their functional roles in viral replication (Chen and Olsthoorn, 2010; Guan et al., 2011, 2012; Kang et al., 2006a; Li et al., 2008; Liu et al., 2007, 2009a; Yang et al., 2011). A detailed understanding of the RNA structures within the *cis*-acting sequences in the 5′UTR and 3′UTR, and eventually the entire MHV genome, and of the RNA–RNA(s), RNA–protein(s) interactions that direct viral RNA synthesis and virus replication will assist our understanding of these processes. Understanding these interactions in highly pathogenic coronaviruses, such as SARS-CoV and MERS-CoV, may enable the design of small molecule inhibitors of these replicative processes.

Acknowledgements

The authors would like to thank Elyse Wudeck for her help in preparing the figures for this work. This work was supported in part by grant 1R01 AI067416 from the U.S. National Institutes of Health and by the CST*R Institute of the Texas A&M Health Science Center.

References

Arbour, N., Cote, G., Lachance, C., Tardieu, M., Cashman, N.R., Talbot, P.J., 1999. Acute and persistent infection of human neural cell lines by human coronavirus OC43. J. Virol. 73 (4), 3338–3350.

Baric, R.S., Nelson, G.W., Fleming, J.O., Deans, R.J., Keck, J.G., Casteel, N., Stohlman, S.A., 1988. Interactions between coronavirus nucleocapsid protein and viral RNAs: implications for viral transcription. J. Virol. 62 (11), 4280–4287.

Baric, R.S., Yount, B., 2000. Subgenomic negative-strand RNA function during mouse hepatitis virus infection. J. Virol. 74 (9), 4039–4046.

Bhardwaj, K., Guarino, L., Kao, C.C., 2004. The severe acute respiratory syndrome coronavirus Nsp15 protein is an endoribonuclease that prefers manganese as a cofactor. J. Virol. 78 (22), 12218–12224.

Bredenbeek, P.J., Pachuk, C.J., Noten, A.F., Charite, J., Luytjes, W., Weiss, S.R., Spaan, W.J., 1990. The primary structure and expression of the second open reading frame of the polymerase gene of the coronavirus MHV-A59; a highly conserved polymerase is expressed by an efficient ribosomal frameshifting mechanism. Nucleic Acids Res. 18 (7), 1825–1832.

Brian, D.A., Baric, R.S., 2005. Coronavirus genome structure and replication. Curr. Top. Microbiol. Immunol. 287, 1–30.

Brockway, S.M., Clay, C.T., Lu, X.T., Denison, M.R., 2003. Characterization of the expression, intracellular localization, and replication complex association of the putative mouse hepatitis virus RNA-dependent RNA polymerase. J. Virol. 77 (19), 10515–10527.

Brockway, S.M., Denison, M.R., 2005. Mutagenesis of the murine hepatitis virus nsp1-coding region identifies residues important for protein processing, viral RNA synthesis, and viral replication. Virology 340 (2), 209–223.

Brown, C.G., Nixon, K.S., Senanayake, S.D., Brian, D.A., 2007. An RNA stem-loop within the bovine coronavirus nsp1 coding region is a *cis*-acting element in defective interfering RNA replication. J. Virol. 81 (14), 7716–7724.

Budzilowicz, C.J., Wilczynski, S.P., Weiss, S.R., 1985. Three intergenic regions of coronavirus mouse hepatitis virus strain A59 genome RNA contain a common nucleotide sequence that is homologous to the 3′ end of the viral mRNA leader sequence. J. Virol. 53 (3), 834–840.

Casais, R., Thiel, V., Siddell, S.G., Cavanagh, D., Britton, P., 2001. Reverse genetics system for the avian coronavirus infectious bronchitis virus. J. Virol. 75 (24), 12359–12369.

Chang, C.K., Hsu, Y.L., Chang, Y.H., Chao, F.A., Wu, M.C., Huang, Y.S., Hu, C.K., Huang, T.H., 2009. Multiple nucleic acid binding sites and intrinsic disorder of severe acute respiratory syndrome coronavirus nucleocapsid protein: implications for ribonucleocapsid protein packaging. J. Virol. 83 (5), 2255–2264.

Chang, R.Y., Hofmann, M.A., Sethna, P.B., Brian, D.A., 1994. A *cis*-acting function for the coronavirus leader in defective interfering RNA replication. J. Virol. 68 (12), 8223–8231.

Chen, S.C., Olsthoorn, R.C., 2010. Group-specific structural features of the 5′-proximal sequences of coronavirus genomic RNAs. Virology 401 (1), 29–41.

Chen, Y., Cai, H., Pan, J., Xiang, N., Tien, P., Ahola, T., Guo, D., 2009. Functional screen reveals SARS coronavirus nonstructural protein nsp14 as a novel cap N7 methyltransferase. Proc. Natl. Acad. Sci. U. S. A. 106 (9), 3484–3489.

Cheng, A., Zhang, W., Xie, Y., Jiang, W., Arnold, E., Sarafianos, S.G., Ding, J., 2005. Expression, purification, and characterization of SARS coronavirus RNA polymerase. Virology 335 (2), 165–176.

Choi, K.S., Huang, P., Lai, M.M., 2002. Polypyrimidine-tract-binding protein affects transcription but not translation of mouse hepatitis virus RNA. Virology 303 (1), 58–68.

Choi, K.S., Mizutani, A., Lai, M.M., 2004. SYNCRIP, a member of the heterogeneous nuclear ribonucleoprotein family, is involved in mouse hepatitis virus RNA synthesis. J. Virol. 78 (23), 13153–13162.

Coleman, C.M., Frieman, M.B., 2014. Coronaviruses: important emerging human pathogens. J. Virol. 88 (10), 5209–5212.

Cologna, R., Hogue, B.G., 2000. Identification of a bovine coronavirus packaging signal. J. Virol. 74 (1), 580–583.

Cologna, R., Spagnolo, J.F., Hogue, B.G., 2000. Identification of nucleocapsid binding sites within coronavirus-defective genomes. Virology 277 (2), 235–249.

Dalton, K., Casais, R., Shaw, K., Stirrups, K., Evans, S., Britton, P., Brown, T.D., Cavanagh, D., 2001. *cis*-acting sequences required for coronavirus infectious bronchitis virus defective-RNA replication and packaging. J. Virol. 75 (1), 125–133.

de Groot, R.J., Baker, S.C., Baric, R.S., Brown, C.S., Drosten, C., Enjuanes, L., Fouchier, R.A., Galiano, M., Gorbalenya, A.E., Memish, Z.A., Perlman, S., Poon, L.L., Snijder, E.J., Stephens, G.M., Woo, P.C., Zaki, A.M., Zambon, M., Ziebuhr, J., 2013. Middle East respiratory syndrome coronavirus (MERS-CoV): announcement of the Coronavirus Study Group. J. Virol. 87 (14), 7790–7792.

de Haan, C.A., Volders, H., Koetzner, C.A., Masters, P.S., Rottier, P.J., 2002. Coronaviruses maintain viability despite dramatic rearrangements of the strictly conserved genome organization. J. Virol. 76 (24), 12491–12502.

Decroly, E., Imbert, I., Coutard, B., Bouvet, M., Selisko, B., Alvarez, K., Gorbalenya, A.E., Snijder, E.J., Canard, B., 2008. Coronavirus nonstructural protein 16 is a cap-0 binding enzyme possessing (nucleoside-2′O)-methyltransferase activity. J. Virol. 82 (16), 8071–8084.

DeDiego, M.L., Alvarez, E., Almazan, F., Rejas, M.T., Lamirande, E., Roberts, A., Shieh, W.J., Zaki, S.R., Subbarao, K., Enjuanes, L., 2007. A severe acute respiratory syndrome coronavirus that lacks the E gene is attenuated in vitro and in vivo. J. Virol. 81 (4), 1701–1713.

Delmas, B., Gelfi, J., L'Haridon, R., Vogel, L.K., Sjostrom, H., Noren, O., Laude, H., 1992. Aminopeptidase N is a major receptor for the enteropathogenic coronavirus TGEV. Nature 357, 417–420.

Drexler, J.F., Corman, V.M., Drosten, C., 2014. Ecology, evolution and classification of bat coronaviruses in the aftermath of SARS. Antiviral Res. 101, 45–56.

Dye, C., Siddell, S.G., 2005. Genomic RNA sequence of Feline coronavirus strain FIPV WSU-79/1146. J. Gen. Virol. 86 (Pt 8), 2249–2253.

Escors, D., Izeta, A., Capiscol, C., Enjuanes, L., 2003. Transmissible gastroenteritis coronavirus packaging signal is located at the 5′ end of the virus genome. J. Virol. 77 (14), 7890–7902.

Fischer, F., Stegen, C.F., Masters, P.S., Samsonoff, W.A., 1998. Analysis of constructed E gene mutants of mouse hepatitis virus confirms a pivotal role for E protein in coronavirus assembly. J. Virol. 72 (10), 7885–7894.

Fosmire, J.A., Hwang, K., Makino, S., 1992. Identification and characterization of a coronavirus packaging signal. J. Virol. 66 (6), 3522–3530.

Galan, C., Sola, I., Nogales, A., Thomas, B., Akoulitchev, A., Enjuanes, L., Almazan, F., 2009. Host cell proteins interacting with the 3′ end of TGEV coronavirus genome influence virus replication. Virology 391 (2), 304–314.

Gerna, G., Passarani, N., Battaglia, M., Rondanelli, E.G., 1985. Human enteric coronaviruses: antigenic relatedness to human coronavirus OC43 and possible etiologic role in viral gastroenteritis. J. Infect. Dis. 151 (5), 796–803.

Goebel, S.J., Hsue, B., Dombrowski, T.F., Masters, P.S., 2004a. Characterization of the RNA components of a putative molecular switch in the 3′ untranslated region of the murine coronavirus genome. J. Virol. 78 (2), 669–682.

Goebel, S.J., Miller, T.B., Bennett, C.J., Bernard, K.A., Masters, P.S., 2007. A hypervariable region within the 3′ *cis*-acting element of the murine coronavirus

genome is nonessential for RNA synthesis but affects pathogenesis. J. Virol. 81 (3), 1274–1287.
Goebel, S.J., Taylor, J., Masters, P.S., 2004b. The 3′ *cis*-acting genomic replication element of the severe acute respiratory syndrome coronavirus can function in the murine coronavirus genome. J. Virol. 78 (14), 7846–7851.
Gorbalenya, A.E., Enjuanes, L., Ziebuhr, J., Snijder, E.J., 2006. Nidovirales: evolving the largest RNA virus genome. Virus Res. 117 (1), 17–37.
Gosert, R., Kanjanahaluethai, A., Egger, D., Bienz, K., Baker, S.C., 2002. RNA replication of mouse hepatitis virus takes place at double-membrane vesicles. J. Virol. 76 (8), 3697–3708.
Grossoehme, N.E., Li, L., Keane, S.C., Liu, P., Dann III, C.E., Leibowitz, J.L., Giedroc, D.P., 2009. Coronavirus N protein N-terminal domain (NTD) specifically binds the transcriptional regulatory sequence (TRS) and melts TRS-cTRS RNA duplexes. J. Mol. Biol. 394 (3), 544–557.
Guan, B.J., Su, Y.P., Wu, H.Y., Brian, D.A., 2012. Genetic evidence of a long-range RNA–RNA interaction between the genomic 5′ untranslated region and the nonstructural protein 1 coding region in murine and bovine coronaviruses. J. Virol. 86 (8), 4631–4643.
Guan, B.J., Wu, H.Y., Brian, D.A., 2011. An optimal *cis*-replication stem-loop IV in the 5′ untranslated region of the mouse coronavirus genome extends 16 nucleotides into open reading frame 1. J. Virol. 85 (11), 5593–5605.
Gustin, K.M., Guan, B.J., Dziduszko, A., Brian, D.A., 2009. Bovine coronavirus nonstructural protein 1 (p28) is an RNA binding protein that binds terminal genomic *cis*-replication elements. J. Virol. 83 (12), 6087–6097.
Hiscox, J.A., Mawditt, K.L., Cavanagh, D., Britton, P., 1995. Investigation of the control of coronavirus subgenomic mRNA transcription by using T7-generated negative-sense RNA transcripts. J. Virol. 69, 6219–6227.
Hofmann, H., Pyrc, K., van der Hoek, L., Geier, M., Berkhout, B., Pöhlmann, S., 2005. Human coronavirus NL63 employs the severe acute respiratory syndrome coronavirus receptor for cellular entry. Proc. Natl. Acad. Sci. U. S. A. 102 (22), 7988–7993.
Holmes, K.V., Lai, M.C., 1996. Coronaviridae: the viruses and their replication. In: Fields, B.N., Knipe, D.M., Howley, P.M., et al. (Eds.), Virology, vol. 1. Lippincott-Raven, Philadelphia, pp. 1075–1093.
Hsue, B., Hartshorne, T., Masters, P.S., 2000. Characterization of an essential RNA secondary structure in the 3′ untranslated region of the murine coronavirus genome. J. Virol. 74 (15), 6911–6921.
Hsue, B., Masters, P.S., 1997. A bulged stem-loop structure in the 3′ untranslated region of the genome of the coronavirus mouse hepatitis virus is essential for replication. J. Virol. 71 (10), 7567–7578.
Huang, P., Lai, M.M., 1999. Polypyrimidine tract-binding protein binds to the complementary strand of the mouse hepatitis virus 3′ untranslated region, thereby altering RNA conformation. J. Virol. 73 (11), 9110–9116.
Huang, P., Lai, M.M., 2001. Heterogeneous nuclear ribonucleoprotein a1 binds to the 3′-untranslated region and mediates potential 5′–3′-end cross talks of mouse hepatitis virus RNA. J. Virol. 75 (11), 5009–5017.
Hurst, K.R., Koetzner, C.A., Masters, P.S., 2009. Identification of in vivo-interacting domains of the murine coronavirus nucleocapsid protein. J. Virol. 83 (14), 7221–7234.
Hurst, K.R., Kuo, L., Koetzner, C.A., Ye, R., Hsue, B., Masters, P.S., 2005. A major determinant for membrane protein interaction localizes to the carboxy-terminal domain of the mouse coronavirus nucleocapsid protein. J. Virol. 79 (21), 13285–13297.
Hurst, K.R., Ye, R., Goebel, S.J., Jayaraman, P., Masters, P.S., 2010. An interaction between the nucleocapsid protein and a component of the replicase-transcriptase complex is crucial for the infectivity of coronavirus genomic RNA. J. Virol. 84 (19), 10276–10288.
Imbert, I., Guillemot, J.C., Bourhis, J.M., Bussetta, C., Coutard, B., Egloff, M.P., Ferron, F., Gorbalenya, A.E., Canard, B., 2006. A second, non-canonical RNA-dependent RNA polymerase in SARS coronavirus. EMBO J. 25 (20), 4933–4942.
Ivanov, K.A., Ziebuhr, J., 2004. Human coronavirus 229E nonstructural protein 13: characterization of duplex-unwinding, nucleoside triphosphatase, and RNA 5′-triphosphatase activities. J. Virol. 78 (14), 7833–7838.
Johnson, R.F., Feng, M., Liu, P., Millership, J.J., Yount, B., Baric, R.S., Leibowitz, J.L., 2005. Effect of mutations in the mouse hepatitis virus 3′(+)42 protein binding element on RNA replication. J. Virol. 79 (23), 14570–14585.
Kang, H., Feng, M., Schroeder, M.E., Giedroc, D.P., Leibowitz, J.L., 2006a. Putative *cis*-acting stem-loops in the 5′ untranslated region of the severe acute respiratory syndrome coronavirus can substitute for their mouse hepatitis virus counterparts. J. Virol. 80 (21), 10600–10614.
Kang, H., Feng, M., Schroeder, M.E., Giedroc, D.P., Leibowitz, J.L., 2006b. Stem-loop 1 in the 5′ UTR of the SARS coronavirus can substitute for its counterpart in mouse hepatitis virus. Adv. Exp. Med. Biol. 581, 105–108.
Keane, S.C., Liu, P., Leibowitz, J.L., Giedroc, D.P., 2012. Functional transcriptional regulatory sequence (TRS) RNA binding and helix destabilizing determinants of murine hepatitis virus (MHV) nucleocapsid (N) protein. J. Biol. Chem. 287 (10), 7063–7073.
Kim, Y.N., Jeong, Y.S., Makino, S., 1993. Analysis of *cis*-acting sequences essential for coronavirus defective interfering RNA replication. Virology 197 (1), 53–63.
Kim, Y.N., Makino, S., 1995. Characterization of a murine coronavirus defective interfering RNA internal *cis*-acting replication signal. J. Virol. 69 (8), 4963–4971.
Knoops, K., Kikkert, M., Worm, S.H., Zevenhoven-Dobbe, J.C., van der Meer, Y., Koster, A.J., Mommaas, A.M., Snijder, E.J., 2008. SARS-coronavirus replication is supported by a reticulovesicular network of modified endoplasmic reticulum. PLoS Biol. 6 (9), e226.
Kuo, L., Masters, P.S., 2003. The small envelope protein E is not essential for murine coronavirus replication. J. Virol. 77 (8), 4597–4608.
Kuo, L., Masters, P.S., 2013. Functional analysis of the murine coronavirus genomic RNA packaging signal. J. Virol. 87 (9), 5182–5192.
Lai, M.M., 1997. RNA–protein interactions in the regulation of coronavirus RNA replication and transcription. Biol. Chem. 378 (6), 477–481.
Lai, M.M., 1998. Cellular factors in the transcription and replication of viral RNA genomes: a parallel to DNA-dependent RNA transcription. Virology 244 (1), 1–12.
Lai, M.M., Baric, R.S., Brayton, P.R., Stohlman, S.A., 1984. Characterization of leader RNA sequences on the virion and mRNAs of mouse hepatitis virus, a cytoplasmic RNA virus. Proc. Natl. Acad. Sci. U. S. A. 81 (12), 3626–3630.
Lai, M.M., Patton, C.D., Baric, R.S., Stohlman, S.A., 1983. Presence of leader sequences in the mRNA of mouse hepatitis virus. J. Virol. 46 (3), 1027–1033.
Laing, C., Schlick, T., 2009. Analysis of four-way junctions in RNA structures. J. Mol. Biol. 390 (3), 547–559.
Lee, C.W., Li, L., Giedroc, D.P., 2011. The solution structure of coronaviral stem-loop 2 (SL2) reveals a canonical CUYG tetraloop fold. FEBS Lett. 585, 1049–1053.
Lee, H.J., Shieh, C.K., Gorbalenya, A.E., Koonin, E.V., La Monica, N., Tuler, J., Bagdzhadzhyan, A., Lai, M.M., 1991. The complete sequence (22 kilobases) of murine coronavirus gene 1 encoding the putative proteases and RNA polymerase. Virology 180 (2), 567–582.
Leibowitz, J.L., Wilhelmsen, K.C., Bond, C.W., 1981. The virus-specific intracellular RNA species of two murine coronaviruses: MHV-a59 and MHV-JHM. Virology 114 (1), 39–51.
Li, H.P., Huang, P., Park, S., Lai, M.M., 1999. Polypyrimidine tract-binding protein binds to the leader RNA of mouse hepatitis virus and serves as a regulator of viral transcription. J. Virol. 73 (1), 772–777.
Li, H.P., Zhang, X., Duncan, R., Comai, L., Lai, M.M., 1997. Heterogeneous nuclear ribonucleoprotein A1 binds to the transcription-regulatory region of mouse hepatitis virus RNA. Proc. Natl. Acad. Sci. U. S. A. 94 (18), 9544–9549.
Li, L., Kang, H., Liu, P., Makkinje, N., Williamson, S.T., Leibowitz, J.L., Giedroc, D.P., 2008. Structural lability in stem-loop 1 drives a 5′ UTR–3′ UTR interaction in coronavirus replication. J. Mol. Biol. 377 (3), 790–803.
Li, W., Moore, M.J., Vasilieva, N., Sui, J., Wong, S.K., Berne, M.A., Somasundaran, M., Sullivan, J.L., Luzuriaga, K., Greenough, T.C., Choe, H., Farzan, M., 2003. Angiotensin-converting enzyme 2 is a functional receptor for the SARS coronavirus. Nature 426 (6965), 450–454.
Lin, Y.J., Lai, M.M., 1993. Deletion mapping of a mouse hepatitis virus defective interfering RNA reveals the requirement of an internal and discontiguous sequence for replication. J. Virol. 67 (10), 6110–6118.
Lin, Y.J., Liao, C.L., Lai, M.M., 1994. Identification of the *cis*-acting signal for minus-strand RNA synthesis of a murine coronavirus: implications for the role of minus-strand RNA in RNA replication and transcription. J. Virol. 68 (12), 8131–8140.
Liu, P., Leibowitz, J.L., 2010. RNA higher-order structures within the Coronavirus 5′ and 3′ untranslated regions and their roles in viral replication. In: Lal, S.K. (Ed.), Molecular biology of the SARS-Coronavirus. Springer, Heidelberg/Dordrecht/London/New York, pp. 47–61.
Liu, P., Li, L., Keane, S.C., Yang, D., Leibowitz, J.L., Giedroc, D.P., 2009a. Mouse hepatitis virus stem-loop 2 adopts a uYNMG(U)a-like tetraloop structure that is highly functionally tolerant of base substitutions. J. Virol. 83 (23), 12084–12093.
Liu, P., Li, L., Millership, J.J., Kang, H., Leibowitz, J.L., Giedroc, D.P., 2007. A U-turn motif-containing stem-loop in the coronavirus 5′ untranslated region plays a functional role in replication. RNA 13 (5), 763–780.
Liu, P., Yang, D., Carter, K., Masud, F., Leibowitz, J.L., 2013. Functional analysis of the stem loop S3 and S4 structures in the coronavirus 3′UTR. Virology 443 (1), 40–47.
Liu, Q., Johnson, R.F., Leibowitz, J.L., 2001. Secondary structural elements within the 3′ untranslated region of mouse hepatitis virus strain JHM genomic RNA. J. Virol. 75 (24), 12105–12113.
Liu, Q., Yu, W., Leibowitz, J.L., 1997. A specific host cellular protein binding element near the 3′ end of mouse hepatitis virus genomic RNA. Virology 232 (1), 74–85.
Liu, Y., Wimmer, E., Paul, A.V., 2009b. *Cis*-acting RNA elements in human and animal plus-strand RNA viruses. Biochim. Biophys. Acta 1789 (9–10), 495–517.
Luytjes, W., Gerritsma, H., Spaan, W.J., 1996. Replication of synthetic defective interfering RNAs derived from coronavirus mouse hepatitis virus-A59. Virology 216 (1), 174–183.
Maeda, J., Repass, J.F., Maeda, A., Makino, S., 2001. Membrane topology of coronavirus E protein. Virology 281 (2), 163–169.
Makino, S., Fujioka, N., Fujiwara, K., 1985. Structure of the intracellular defective viral RNAs of defective interfering particles of mouse hepatitis virus. J. Virol. 54 (2), 329–336.
Makino, S., Joo, M., Makino, J.K., 1991. A system for study of coronavirus mRNA synthesis: a regulated, expressed subgenomic defective interfering RNA results from intergenic site insertion. J. Virol. 65 (11), 6031–6041.
Makino, S., Shieh, C.K., Soe, L.H., Baker, S.C., Lai, M.M., 1988. Primary structure and translation of a defective interfering RNA of murine coronavirus. Virology 166 (2), 550–560.
Makino, S., Yokomori, K., Lai, M.M., 1990. Analysis of efficiently packaged defective interfering RNAs of murine coronavirus: localization of a possible RNA-packaging signal. J. Virol. 64 (12), 6045–6053.
Marra, M.A., Jones, S.J., Astell, C.R., Holt, R.A., Brooks-Wilson, A., Butterfield, Y.S., Khattra, J., Asano, J.K., Barber, S.A., Chan, S.Y., Cloutier, A., Coughlin, S.M., Freeman, D., Girn, N., Griffith, O.L., Leach, S.R., Mayo, M., McDonald, H., Montgomery, S.B., Pandoh, P.K., Petrescu, A.S., Robertson, A.G., Schein, J.E., Siddiqui, A., Smailus, D.E., Stott, J.M., Yang, G.S., Plummer, F., Andonov, A., Artsob, H., Bastien, N.,

Bernard, K., Booth, T.F., Bowness, D., Czub, M., Drebot, M., Fernando, L., Flick, R., Garbutt, M., Gray, M., Grolla, A., Jones, S., Feldmann, H., Meyers, A., Kabani, A., Li, Y., Normand, S., Stroher, U., Tipples, G.A., Tyler, S., Vogrig, R., Ward, D., Watson, B., Brunham, R.C., Krajden, M., Petric, M., Skowronski, D.M., Upton, C., Roper, R.L., 2003. The genome sequence of the SARS-associated coronavirus. Science 300 (5624), 1399–1404.

Masters, P.S., 2006. The molecular biology of coronaviruses. Adv. Virus Res. 66, 193–292.

Mateos-Gomez, P.A., Morales, L., Zuniga, S., Enjuanes, L., Sola, I., 2013. Long-distance RNA–RNA interactions in the coronavirus genome form high-order structures promoting discontinuous RNA synthesis during transcription. J. Virol. 87 (1), 177–186.

Mathews, D.H., Disney, M.D., Childs, J.L., Schroeder, S.J., Zuker, M., Turner, D.H., 2004. Incorporating chemical modification constraints into a dynamic programming algorithm for prediction of RNA secondary structure. Proc. Natl. Acad. Sci. U. S. A. 101 (19), 7287–7292.

McRoy, W.C., Baric, R.S., 2008. Amino acid substitutions in the S2 subunit of mouse hepatitis virus variant V51 encode determinants of host range expansion. J. Virol. 82 (3), 1414–1424.

Mendez, A., Smerdou, C., Izeta, A., Gebauer, F., Enjuanes, L., 1996. Molecular characterization of transmissible gastroenteritis coronavirus defective interfering genomes: packaging and heterogeneity. Virology 217 (2), 495–507.

Minskaia, E., Hertzig, T., Gorbalenya, A.E., Campanacci, V., Cambillau, C., Canard, B., Ziebuhr, J., 2006. Discovery of an RNA virus 3′→5′ exoribonuclease that is critically involved in coronavirus RNA synthesis. Proc. Natl. Acad. Sci. U. S. A. 103 (13), 5108–5113.

Morales, L., Mateos-Gomez, P.A., Capiscol, C., del Palacio, L., Enjuanes, L., Sola, I., 2013. Transmissible gastroenteritis coronavirus genome packaging signal is located at the 5′ end of the genome and promotes viral RNA incorporation into virions in a replication-independent process. J. Virol. 87 (21), 11579–11590.

Murray, R.S., Brown, B., Brian, D., Cabirac, G.F., 1992. Detection of coronavirus RNA and antigen in multiple sclerosis brain. Ann. Neurol. 31 (5), 525–533.

Nanda, S.K., Johnson, R.F., Liu, Q., Leibowitz, J.L., 2004. Mitochondrial HSP70, HSP40, and HSP60 bind to the 3′ untranslated region of the Murine hepatitis virus genome. Arch. Virol 149 (1), 93–111.

Nanda, S.K., Leibowitz, J.L., 2001. Mitochondrial aconitase binds to the 3′ untranslated region of the mouse hepatitis virus genome. J. Virol. 75 (7), 3352–3362.

Narayanan, K., Chen, C.J., Maeda, J., Makino, S., 2003. Nucleocapsid-independent specific viral RNA packaging via viral envelope protein and viral RNA signal. J. Virol. 77 (5), 2922–2927.

Nash, T.C., Buchmeier, M.J., 1997. Entry of mouse hepatitis virus into cells by endosomal and nonendosomal pathways. Virology 233 (1), 1–8.

Nelson, G.W., Stohlman, S.A., Tahara, S.M., 2000. High affinity interaction between nucleocapsid protein and leader/intergenic sequence of mouse hepatitis virus RNA. J. Gen. Virol. 81 (Pt 1), 181–188.

Pasternak, A.O., van den Born, E., Spaan, W.J., Snijder, E.J., 2003. The stability of the duplex between sense and antisense transcription-regulating sequences is a crucial factor in arterivirus subgenomic mRNA synthesis. J. Virol. 77 (2), 1175–1183.

Pinon, J.D., Teng, H., Weiss, S.R., 1999. Further requirements for cleavage by the murine coronavirus 3C-like proteinase: identification of a cleavage site within ORF1b. Virology 263 (2), 471–484.

Putics, A., Filipowicz, W., Hall, J., Gorbalenya, A.E., Ziebuhr, J., 2005. ADP-ribose-1-monophosphatase: a conserved coronavirus enzyme that is dispensable for viral replication in tissue culture. J. Virol. 79 (20), 12721–12731.

Raj, V.S., Mou, H., Smits, S.L., Dekkers, D.H., Muller, M.A., Dijkman, R., Muth, D., Demmers, J.A., Zaki, A., Fouchier, R.A., Thiel, V., Drosten, C., Rottier, P.J., Osterhaus, A.D., Bosch, B.J., Haagmans, B.L., 2013. Dipeptidyl peptidase 4 is a functional receptor for the emerging human coronavirus-EMC. Nature 495 (7440), 251–254.

Raman, S., Bouma, P., Williams, G.D., Brian, D.A., 2003. Stem-loop III in the 5′ untranslated region is a *cis*-acting element in bovine coronavirus defective interfering RNA replication. J. Virol. 77 (12), 6720–6730.

Raman, S., Brian, D.A., 2005. Stem-loop IV in the 5′ untranslated region is a *cis*-acting element in bovine coronavirus defective interfering RNA replication. J. Virol. 79 (19), 12434–12446.

Resta, S., Luby, J.P., Rosenfeld, C.R., Siegel, J.D., 1985. Isolation and propagation of a human enteric coronavirus. Science 229 (4717), 978–981.

Rota, P.A., Oberste, M.S., Monroe, S.S., Nix, W.A., Campagnoli, R., Icenogle, J.P., Penaranda, S., Bankamp, B., Maher, K., Chen, M.H., Tong, S., Tamin, A., Lowe, L., Frace, M., DeRisi, J.L., Chen, Q., Wang, D., Erdman, D.D., Peret, T.C., Burns, C., Ksiazek, T.G., Rollin, P.E., Sanchez, A., Liffick, S., Holloway, B., Limor, J., McCaustland, K., Olsen-Rasmussen, M., Fouchier, R., Gunther, S., Osterhaus, A.D., Drosten, C., Pallansch, M.A., Anderson, L.J., Bellini, W.J., 2003. Characterization of a novel coronavirus associated with severe acute respiratory syndrome. Science 300 (5624), 1394–1399.

Rousset, S., Moscovici, O., Lebon, P., Barbet, J.P., Helardot, P., Mace, B., Bargy, F., Le Tan, V., Chany, C., 1984. Intestinal lesions containing coronavirus-like particles in neonatal necrotizing enterocolitis: an ultrastructural analysis. Pediatrics 73 (2), 218–224.

Sawicki, S.G., Sawicki, D.L., 1990. Coronavirus transcription: subgenomic mouse hepatitis virus replicative intermediates function in RNA synthesis. J. Virol. 64 (3), 1050–1056.

Sawicki, S.G., Sawicki, D.L., 1998. A new model for coronavirus transcription. Adv. Exp. Med. Biol. 440, 215–219.

Schiller, J.J., Kanjanahaluethai, A., Baker, S.C., 1998. Processing of the coronavirus MHV-JHM polymerase polyprotein: identification of precursors and proteolytic products spanning 400 kilodaltons of ORF1a. Virology 242 (2), 288–302.

Sethna, P.B., Hung, S.L., Brian, D.A., 1989. Coronavirus subgenomic minus-strand RNAs and the potential for mRNA replicons. Proc. Natl. Acad. Sci. U. S. A. 86 (14), 5626–5630.

Shen, X., Masters, P.S., 2001. Evaluation of the role of heterogeneous nuclear ribonucleoprotein A1 as a host factor in murine coronavirus discontinuous transcription and genome replication. Proc. Natl. Acad. Sci. U. S. A. 98 (5), 2717–2722.

Shi, S.T., Yu, G.Y., Lai, M.M., 2003. Multiple type A/B heterogeneous nuclear ribonucleoproteins (hnRNPs) can replace hnRNP A1 in mouse hepatitis virus RNA synthesis. J. Virol. 77 (19), 10584–10593.

Snijder, E.J., Bredenbeek, P.J., Dobbe, J.C., Thiel, V., Ziebuhr, J., Poon, L.L., Guan, Y., Rozanov, M., Spaan, W.J., Gorbalenya, A.E., 2003. Unique and conserved features of genome and proteome of SARS-coronavirus, an early split-off from the coronavirus group 2 lineage. J. Mol. Biol. 331 (5), 991–1004.

Sola, I., Moreno, J.L., Zuniga, S., Alonso, S., Enjuanes, L., 2005. Role of nucleotides immediately flanking the transcription-regulating sequence core in coronavirus subgenomic mRNA synthesis. J. Virol. 79 (4), 2506–2516.

Sonenberg, N., 1996. mRNA 5′ cap binding protein eIF4E and control of cell growth. In: Hershey, J.W.B., M, M.B., Sonenberg, N. (Eds.), Translational Control. Cold Spring Harbor Laboratory Press, Cold Spring Harbor, NY, pp. 245–270.

Sonenberg, N., Morgan, M.A., Merrick, W.C., Shatkin, A.J., 1978. A polypeptide in eukaryotic initiation factors that crosslinks specifically to the 5′-terminal cap in mRNA. Proc. Natl. Acad. Sci. U. S. A. 75 (10), 4843–4847.

Spaan, W.J., Rottier, P.J., Horzinek, M.C., van der Zeijst, B.A., 1982. Sequence relationships between the genome and the intracellular RNA species 1, 3, 6, and 7 of mouse hepatitis virus strain A59. J. Virol. 42 (2), 432–439.

Spagnolo, J.F., Hogue, B.G., 2000. Host protein interactions with the 3′ end of bovine coronavirus RNA and the requirement of the poly(A) tail for coronavirus defective genome replication. J. Virol. 74 (11), 5053–5065.

Stadler, K., Masignani, V., Eickmann, M., Becker, S., Abrignani, S., Klenk, H.D., Rappuoli, R., 2003. SARS – beginning to understand a new virus. Nat. Rev. Microbiol. 1 (3), 209–218.

Stammler, S.N., Cao, S., Chen, S.J., Giedroc, D.P., 2011. A conserved RNA pseudoknot in a putative molecular switch domain of the 3′-untranslated region of coronaviruses is only marginally stable. RNA 17 (9), 1747–1759.

Stohlman, S.A., Baric, R.S., Nelson, G.N., Soe, L.H., Welter, L.M., Deans, R.J., 1988. Specific interaction between coronavirus leader RNA and nucleocapsid protein. J. Virol. 62 (11), 4288–4295.

Tahara, S.M., Dietlin, T.A., Nelson, G.W., Stohlman, S.A., Manno, D.J., 1998. Mouse hepatitis virus nucleocapsid protein as a translational effector of viral mRNAs. Adv. Exp. Med. Biol. 440, 313–318.

van der Most, R.G., Bredenbeek, P.J., Spaan, W.J., 1991. A domain at the 3′ end of the polymerase gene is essential for encapsidation of coronavirus defective interfering RNAs. J. Virol. 65 (6), 3219–3226.

van der Most, R.G., de Groot, R.J., Spaan, W.J.M., 1994. Subgenomic RNA synthesis directed by a synthetic defective interfering RNA of Mouse Hepatitis Virus: a study of coronavirus transcription initiation. J. Virol. 68, 3656–3666.

van Marle, G., Dobbe, J.C., Gultyaev, A.P., Luytjes, W., Spaan, W.J., Snijder, E.J., 1999. Arterivirus discontinuous mRNA transcription is guided by base pairing between sense and antisense transcription-regulating sequences. Proc. Natl. Acad. Sci. U. S. A. 96 (21), 12056–12061.

Wang, H., Yang, P., Liu, K., Guo, F., Zhang, Y., Zhang, G., Jiang, C., 2008. SARS coronavirus entry into host cells through a novel clathrin- and caveolae-independent endocytic pathway. Cell Res. 18 (2), 290–301.

Weiss, S.R., Hughes, S.A., Bonilla, P.J., Turner, J.D., Leibowitz, J.L., Denison, M.R., 1994. Coronavirus polyprotein processing. Arch. Virol. Suppl. 9, 349–358.

Weiss, S.R., Leibowitz, J.L., 2007. Pathogenesis of murine coronavirus infections. In: Perlman, S., Gallagher, T., Snijder, E.J. (Eds.), Nidoviruses. ASM Press, Washington, DC, pp. 259–278.

Williams, G.D., Chang, R.Y., Brian, D.A., 1999. A phylogenetically conserved hairpin-type 3′ untranslated region pseudoknot functions in coronavirus RNA replication. J. Virol. 73 (10), 8349–8355.

Williams, R.K., Jiang, G.S., Holmes, K.V., 1991. Receptor for mouse hepatitis virus is a member of the carcinoembryonic antigen family of glycoproteins. Proc. Natl. Acad. Sci. U. S. A. 88 (13), 5533–5536.

Wu, H.Y., Guan, B.J., Su, Y.P., Fan, Y.H., Brian, D.A., 2014. Reselection of a genomic upstream open reading frame in mouse hepatitis coronavirus 5′-untranslated-region mutants. J. Virol. 88 (2), 846–858.

Wu, H.Y., Guy, J.S., Yoo, D., Vlasak, R., Urbach, E., Brian, D.A., 2003. Common RNA replication signals exist among group 2 coronaviruses: evidence for in vivo recombination between animal and human coronavirus molecules. Virology 315 (1), 174–183.

Yang, D., Liu, P., Giedroc, D.P., Leibowitz, J., 2011. Mouse hepatitis virus stem-loop 4 functions as a spacer element required to drive subgenomic RNA synthesis. J. Virol. 85 (17), 9199–9209.

Yang, D., Liu, P., Wudeck, E.V., Giedroc, D.P., Leibowitz, J.L., 2015. SHAPE analysis of the RNA secondary structure of the Mouse Hepatitis Virus 5′ untranslated region and N-terminal nsp1 coding sequences. Virology 475, 15–27.

Yeager, C.L., Ashmun, R.A., Williams, R.K., Cardellichio, C.B., Shapiro, L.H., Look, A.T., Holmes, K.V., 1992. Human aminopeptidase N is a receptor for human coronavirus. Nature 357, 420–422.

Yount, B., Curtis, K.M., Baric, R.S., 2000. Strategy for systematic assembly of large RNA and DNA genomes: transmissible gastroenteritis virus model. J. Virol. 74 (22), 10600–10611.

Yu, W., Leibowitz, J.L., 1995a. A conserved motif at the 3′ end of mouse hepatitis virus genomic RNA required for host protein binding and viral RNA replication. Virology 214 (1), 128–138.
Yu, W., Leibowitz, J.L., 1995b. Specific binding of host cellular proteins to multiple sites within the 3′ end of mouse hepatitis virus genomic RNA. J. Virol. 69 (4), 2016–2023.
Zaki, A.M., van Boheemen, S., Bestebroer, T.M., Osterhaus, A.D., Fouchier, R.A., 2012. Isolation of a novel coronavirus from a man with pneumonia in Saudi Arabia. N. Engl. J. Med. 367 (19), 1814–1820.
Ziebuhr, J., Snijder, E.J., Gorbalenya, A.E., 2000. Virus-encoded proteinases and proteolytic processing in the Nidovirales. J. Gen. Virol. 81 (Pt 4), 853–879.
Zuniga, S., Cruz, J.L., Sola, I., Mateos-Gomez, P.A., Palacio, L., Enjuanes, L., 2010. Coronavirus nucleocapsid protein facilitates template switching and is required for efficient transcription. J. Virol. 84 (4), 2169–2175.
Zuniga, S., Sola, I., Alonso, S., Enjuanes, L., 2004. Sequence motifs involved in the regulation of discontinuous coronavirus subgenomic RNA synthesis. J. Virol. 78 (2), 980–994.
Zuniga, S., Sola, I., Moreno, J.L., Sabella, P., Plana-Duran, J., Enjuanes, L., 2007. Coronavirus nucleocapsid protein is an RNA chaperone. Virology 357 (2), 215–227.
Zust, R., Miller, T.B., Goebel, S.J., Thiel, V., Masters, P.S., 2008. Genetic interactions between an essential 3′ *cis*-acting RNA pseudoknot, replicase gene products, and the extreme 3′ end of the mouse coronavirus genome. J. Virol. 82 (3), 1214–1228.